T.C.

AKDENIZ UNIVERSITY

FUNCTIONAL CHARACTERIZATION OF THE *PdZIP8* GENE AND ITS ROLE IN ZINC UPTAKE IN *Arabidopsis thaliana*

Beyza YÜKSEL

INSTITUTE OF NATURAL SCIENCES

DEPARTMENT OF AGRICULTURAL BIOTECHNOLOGY

MASTER THESIS

AUGUST 2025

ANTALYA

T.C.

AKDENIZ UNIVERSITY

FUNCTIONAL CHARACTERIZATION OF THE *PdZIP8* GENE AND ITS ROLE IN ZINC UPTAKE IN *Arabidopsis thaliana*

Beyza YÜKSEL

INSTITUTE OF NATURAL SCIENCES

DEPARTMENT OF AGRICULTURAL BIOTECHNOLOGY

MASTER THESIS

AUGUST 2025

ANTALYA

T.C.

AKDENİZ UNIVERSITY

INSTITUTE OF NATURAL SCIENCES

FUNCTIONAL CHARACTERIZATION OF THE *PdZIP8* GENE AND ITS ROLE IN ZINC UPTAKE IN *Arabidopsis thaliana*

Beyza YÜKSEL

INSTITUTE OF NATURAL SCIENCES

DEPARTMENT OF AGRICULTURAL BIOTECHNOLOGY

MASTER THESIS

This master thesis funded by BAP project ID FYL-2024-6575

AUGUST 2025

T.C.

AKDENİZ UNIVERSITY

INSTITUTE OF NATURAL SCIENCES

FUNCTIONAL CHARACTERIZATION OF THE *PdZIP8* GENE AND ITS ROLE IN ZINC UPTAKE IN *Arabidopsis thaliana*

Beyza YÜKSEL

INSTITUTE OF NATURAL SCIENCES

DEPARTMENT OF AGRICULTURAL BIOTECHNOLOGY

MASTER THESIS

This thesis was unanimously accepted by the jury on 11/07/2025.

Assoc. Prof. Dr. M. Aydın AKBUDAK

Assoc. Prof. Dr. Aysun ÖZÇELİK

Assoc. Prof. Dr. Ali Tevfik UNCU

ÖZET

PdZIP8 GENİNİN FONKSİYONEL KARAKTERİZASYONU VE *Arabidopsis thaliana'*da ÇİNKO ALIMINDA ROLÜ

Beyza YÜKSEL

Yüksek Lisans Tezi, Tarımsal Biyoteknoloji Anabilim Dalı

Danışman: Doç. Dr. M. Aydın AKBUDAK

Ağustos 2025; 52 sayfa

Çinko eksikliği, dünya genelinde yaygınlık açısından demir eksikliğinin ardından en sık görülen ikinci mikro element eksikliğidir. Türkiye'de ise en yaygın mikro element eksikliği olarak öne çıkmaktadır. İnsan ve hayvan sağlığı üzerinde ciddi sorunlara ve ölümlere yol açarken, bitkilerde büyümeyi sınırlandıran ve tarımsal üretimi kısıtlayan önemli bir abiyotik stres faktörüdür. Çinko eksikliği, üretilen ürünlerin veriminde ve kalitesinde ciddi düşüşlere neden olmaktadır.

Dünya genelinde tarım topraklarının yaklaşık yarısı çinko açısından yetersizdir. Ancak bazı durumlarda, toprakta yeterli miktarda çinko bulunsa dahi toprak özellikleri, bitkilerin çinkoyu etkin bir şekilde ve yeterli miktarda almasını engelleyebilmektedir. Bu nedenle, bitkilerde çinko alım mekanizmasının aydınlatılması ve çinko alımıyla ilişkili genlerin tanımlanması büyük önem taşımaktadır.

Bu çalışmada, *Puccinellia distans*'ta tanımlanan çinko-demir düzenleyici *ZIP8* geninin çinko alım fonksiyonunun belirlenmesi amaçlanmıştır. Yapılan analizler sonucunda, *PdZIP8* genini taşıyan çinko mutant *Saccharomyces cerevisiae* hücrelerinin 200 µM EDTA ve 20 mM EGTA içeren çinko yetersizliği koşullarını tolere ederek hayatta kalabildiği, ancak bu geni taşımayan hücrelerin aynı koşullarda büyüyemediği ortaya konulmuştur. Bununla birlikte, *PdZIP8* genini aşırı ifadeleyen *Arabidopsis thaliana* hatlarında gerçekleştirilen fenotipik analizler, RT-qPCR ve ICP-MS sonuçları, *PdZIP8* geninin çinko alımı ile ilişkili olduğunu güçlü bir şekilde desteklemektedir. Çalışmada karakterizasyonu yapılan bu genin, bitkilerde çinko içeriğini artırmaya yönelik çeşitli ıslah programlarında potansiyel olarak kullanılabileceği öngörülmektedir.

ANAHTAR KELİMELER: Arabidopsis, Çinko Eksikliği, Çinko Taşıyıcıları, Maya, *Puccinellia distans*, Şelatlama, ZIP8

JÜRİ: Doç. Dr. M. Aydın AKBUDAK

Doç. Dr. Aysun ÖZÇELİK

Doç. Dr. Ali Tevfik UNCU

ABSTRACT

FUNCTIONAL CHARACTERIZATION OF THE *PdZIP8* GENE AND ITS ROLE IN ZINC UPTAKE IN *Arabidopsis thaliana*

Beyza YÜKSEL

MSc Thesis in the Department of Agricultural Biotechnology

Supervisor: Assoc. Prof. Dr. M. Aydın AKBUDAK

August 2025; 52 pages

Zinc deficiency is the second prevalent microelement deficiency in the world following iron deficiency. It is the most prevalent microelement deficiency in Turkey. This deficiency is one of the significant abiotic stress factors that cause serious health issues and deaths in humans and animals, while also restricting growth and agricultural production in plants. Zinc deficiency leads to critical decreases in the yield and quality of crops. Moreover, almost half of the world's soils are deficient in zinc. In some cases, even when the zinc content in the soil is sufficient, soil characteristics can prevent plants from absorbing zinc effectively and in the required amount. For these reasons, elucidating the zinc uptake mechanism in plants and identifying the genes associated with zinc absorption has great importance.

This study aimed to reveal the zinc uptake function of the *ZIP8* gene, identified as a zinc-iron regulator in *Puccinellia distans*. It has been demonstrated that zinc mutant yeast cells containing the *PdZIP8* gene can tolerate and survive in zinc deficient conditions with 200 µM EDTA and 20 mM EGTA, while cells lacking the gene cannot grow under these conditions. Additionally, phenotypic analyses conducted in *Arabidopsis thaliana* lines overexpressing the *PdZIP8*, along with RT-qPCR and ICP-MS results, further emphasize the association of the *PdZIP8* with zinc uptake. It is anticipated that the characterization of the studied gene will be used in various breeding programs aimed at enhancing zinc content in plants.

KEYWORDS: Arabidopsis, Chelating, *Puccinellia distans*, Yeast, Zinc Deficiency, ZIP8, Zinc Transporters

COMMITTEE: Assoc. Prof. Dr. M. Aydın AKBUDAK

Assoc. Prof. Dr. Aysun ÖZÇELİK

Assoc. Prof. Dr. Ali Tevfik UNCU

ACKNOWLEDGEMENTS

I would like to express my deepest gratitude to my supervisor, Assoc. Prof. Dr. M. Aydın AKBUDAK, for his valuable guidance, support, and encouragement throughout my research journey. His expertise and insights have significantly shaped my study and inspired me to pursue excellence.

I would also like to thank the lab members for their companionship and assistance. In particular, I am thankful to Şeyma Nur ERDEĞER ÇOLAK and Kübra BUDAK TEK for their willingness to share their knowledge and provide valuable feedback. Their support helped me navigate the challenges along the way, and I truly appreciate it.

Special thanks to Eylül Bilge SARI and Ahmet İKTEN. Their support made the tough moments feel lighter and the entire journey more enjoyable. I couldn't have asked for better colleagues.

I am also deeply grateful to my parents, Yurdanur and Cüneyt YÜKSEL for their unwavering love, patience, and encouragement. Their belief in me has been my greatest source of strength.

TABLE OF CONTENTS

ACADEMIC DECLARATION

I declare that the Master's thesis entitled *"*Functional Characterization of the PdZIP8 Gene and Its Role in Zinc Uptake in *Arabidopsis thaliana"* has been written in accordance with academic rules and ethical standards. I affirm that all information and content that is not my own has been properly cited and referenced throughout the thesis.

…/…/….

Beyza YÜKSEL

LIST OF SYMBOLS AND ABBREVIATIONS

Symbols

µg : microgram

µl : microliter

% : percent

bp : base pair

kb : kilobase

g : gram

mg : milligram

ng : nanogram

ml : milliliter

mM : millimolar

µM : micromolar

µF : microfarad

s : second

V : volt

dH_2O : distilled water

rpm : revolutions per minute

°C : centigrade degree

. : decimal point

Zn : zinc

Fe : iron

Mn : manganese

Ni : nickel

Cu : copper

Cd : cadmium

Se : selenium

EtOH : ethanol

Ura : uracil

\+ : plus

/ : division

= : equality

Ω : ohm

Δ : delta

Abbreviations:

ANOVA : Analysis of variance

CDF : Cation Diffusion Facilitators

CSM : Complete Supplement Mixture

DNA : Deoxyribonucleic acid

EV : Empty Vector

ICP : Inductively Coupled Plasma

LB : Luria-Bertani

MS : Murashige and Skoog

NRAMP : Natural Resistance Associated Macrophage Proteins

OD : Optical Density

ORF : Open Reading Frame

PCR : Polymerase Chain Reaction

RNA : Ribonucleicacid

RT-PCR : Real Time Polymerase Chain Reaction

YNB : Yeast Nitrogen Base

YPD : Yeast Peptone Dextrose

ZIP : Zinc Induced Iron Induced Transporter

LIST OF FIGURES

LIST OF TABLES

1. INTRODUCTION

Zinc (Zn) is an essential micronutrient required for the growth and development of all life forms. Although needed in trace amounts, zinc plays a critical role in various physiological processes, including gene regulation, membrane integrity, protein synthesis, reproduction, photosynthesis, and the production of growth regulators (Kumar 2016). Zinc deficiency leads to severe health problems in humans, such as growth retardation, skin disorders, and impaired reproduction (Hambridge 2000). In plants, it causes stunted growth, leaf chlorosis, reduced fruit size, and immature shoot development (Krishna 2020). Cereal grains, which serve as staple foods worldwide, are particularly susceptible to zinc deficiency, making it both an economic and global health concern (Çakmak 2008). It is estimated that approximately 50 % of the world's agricultural soils are zinc-deficient (Deshpande 2018). Even when zinc fertilizers and supplements are applied, soil properties often limit zinc bioavailability, preventing plants from efficiently absorbing the element (Kumar 2016).

Plants absorb zinc as Zn^{2+} through their roots, after which zinc ions are transported via xylem to various tissues. However, due to the inability of zinc ions to passively diffuse across cell membranes, specialized transporter proteins are required for uptake (Guerinot 1999). The ZIP (Zinc-regulated/Iron-regulated Transporter-like Protein) family is one of the most well-characterized groups of transporters responsible for zinc uptake and homeostasis in plants. Besides zinc, ZIP transporters can also facilitate the movement of iron (Fe), cadmium (Cd), and manganese (Mn). The ZIP family was first identified and characterized in *Arabidopsis thaliana* (Grotz et al. 1998), and to date, over 100 ZIP transporters have been reported across various plant species, including wheat, barley, maize, rice, and soybean.

This study aimed to elucidate the zinc uptake function of the *PdZIP8* gene, which was previously identified in *Puccinellia distans*, a hyperaccumulator species. To achieve this, two model organisms, *Saccharomyces cerevisiae* (baker's yeast) and *Arabidopsis thaliana* (Thale cress), were utilized due to their rapid growth and ease of genetic manipulation. The *PdZIP8* gene was cloned into the yeast expression vector pAG426GPD and introduced into the wild-type yeast strain W303 and the zinc uptake-deficient double mutant strain ZHY3 (*zrt1*/*zrt2*). A yeast complementation assay was performed under zinc-deficient conditions using EDTA and EGTA as chelating agents to assess *PdZIP8* function in zinc uptake.

To further investigate subcellular localization, the *PdZIP8* gene was fused with GFP (PdZIP8-EGFP) in the pAG426GPD-EGFP vector and transformed into ZHY3 yeast cells, followed by confocal microscopy imaging. Additionally, previously generated *A. thaliana* transgenic lines overexpressing *PdZIP8* (pGFPGUSPlus-PdZIP8) were analyzed for zinc content using inductively coupled plasma mass spectrometry (ICP-MS). Gene expression levels in these lines were quantified via RT-qPCR, and phenotypic assessments, including measurements of root and shoot length, fresh and dry weight, and chlorophyll content analyses, were conducted to validate the functional implications.

Results indicated that *PdZIP8* expression in *A. thaliana* was transcriptionally induced under zinc-deficient conditions. Furthermore, *PdZIP8* was able to rescue the

zinc uptake deficiency in yeast mutants, highlighting its critical role in zinc acquisition. These findings provide novel insights into the molecular mechanisms underlying zinc homeostasis and suggest that *PdZIP8* could be a promising target for biofortification strategies aimed at improving zinc content in crops with inherently low zinc levels, thereby enhancing agricultural productivity and nutritional quality on a global scale.

2. LITERATURE REVIEW

2.1. Zinc (Zn) as an Essential Element

Zinc (Zn), a transition metal with an atomic number of 30, plays a crucial role in biological systems. Raulin (1869) was the first to report that *Aspergillus niger* could not grow in the absence of zinc, highlighting its importance in microbial development. Since then, numerous studies have confirmed that zinc is an essential trace element required for the growth and functioning of living organisms (Prasad 1978).

2.2. Physiological Functions of Zinc

Zinc plays a vital role in numerous physiological processes, serving both structural and regulatory functions. As a cofactor, it is essential for the activity of over 300 enzymes, influencing key metabolic pathways (McCall et al. 2000). Additionally, zinc contributes to cell membrane stability and integrity, protecting cells from oxidative damage caused by reactive oxygen species (ROS).

In plants, zinc is crucial for phytohormone biosynthesis, particularly indole-3-acetic acid (IAA), a key auxin that regulates growth and development (Marschner 1997; Kumar 2016). Research has shown that IAA concentrations in the shoots and leaves of bean plants grown in zinc-deficient conditions are approximately 50% lower than in those cultivated with sufficient zinc (Çakmak et al. 1989). Furthermore, zinc facilitates the synthesis of chlorophyll and carbohydrates, including sucrose and starch, establishing a strong correlation between zinc availability and photosynthetic efficiency. Studies indicate that plant species such as sugarcane, maize, and sorghum experience impaired photosynthetic carbon metabolism under zinc deficiency (Kumar 2016). Beyond its metabolic functions, zinc is also essential for reproductive success in plants, playing a critical role in the formation of anthers, pollen, and seeds.

2.3. The Effects of Zinc Deficiency

Zinc is an essential element for the growth and development of all organisms, and its deficiency poses a significant global concern. It is the second most widespread micronutrient deficiency worldwide, following iron deficiency (Graham and Welch 2012). In humans, blood zinc levels below 70 mcg/dL are classified as deficient, leading to various health complications. Common clinical symptoms of zinc deficiency include growth retardation, alopecia, dermatological disorders, reproductive impairments, delayed wound healing, and, in severe cases, increased mortality. The risk is particularly high in populations with cereal-based diets, as cereals generally have low zinc content. An estimated 3 billion people worldwide suffer from health issues linked to inadequate zinc intake (Yokolawa et al. 2024).

In plants, zinc levels between 30 and 100 g^{-1} dry weight (DW) are considered sufficient for optimal growth, while concentrations below 30 g^{-1} DW indicate zinc deficiency (Marschner 1995; Van de Mortel et al. 2006). Deficient plants exhibit symptoms such as stunted growth, shortened internodes, partial chlorosis, and poor root, shoot, and leaf development. Additionally, zinc deficiency negatively impacts

reproductive structures, leading to reduced fruit, anther, and seed formation, ultimately affecting both crop quality and yield.

Ensuring an adequate supply of zinc in the soil is critical for maintaining agricultural productivity. However, approximately 50% of the world's agricultural soils are classified as zinc-deficient, posing a major challenge to global food security (FAO 2000). In Türkiye, zinc deficiency is a significant concern, with 49.8% of soils (approximately 14 million hectares) classified as zinc-deficient (Eyüpoğlu et al. 1996). This issue is particularly prevalent in calcareous and sandy soils, which are characterized by high pH levels and elevated phosphorus content, both of which limit zinc availability to plants (Marschner 1995).

A common strategy to mitigate zinc deficiency is the application of zinc-containing fertilizers. However, this approach provides only a temporary solution, as the high market prices of these fertilizers often make them unaffordable for many farmers, limiting their widespread and consistent use (Krishna 2020). Sustainable and cost-effective alternatives, such as biofortification and improved agronomic practices, are essential for addressing this challenge in the long term.

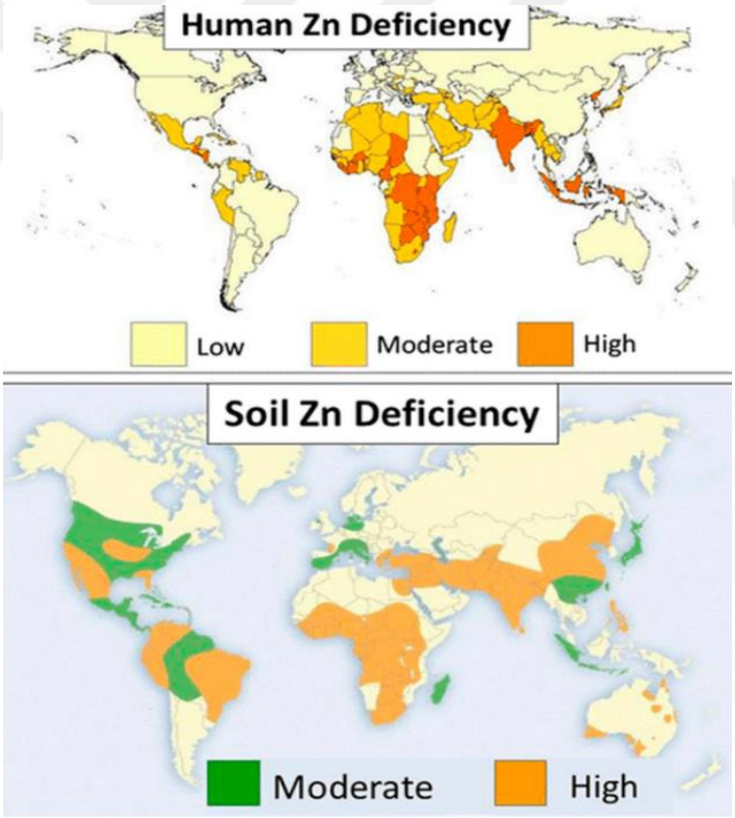

Figure 2.1. A global overview of zinc deficiency in humans and soils (Adapted from Alloway 2011)

2.4. Zn Uptake Mechanism in Plants

Despite adequate zinc concentrations in soils, its bioavailability to plants remains limited. Approximately 90% of the total soil zinc is considered unavailable for plant uptake (Mandal et al. 1988). Although zinc-based fertilizers are commonly used to supplement plant nutrition, their effectiveness is often constrained by various soil properties, including soil type, structure, and matrix composition, which further restrict zinc bioavailability (Çakmak 2008).

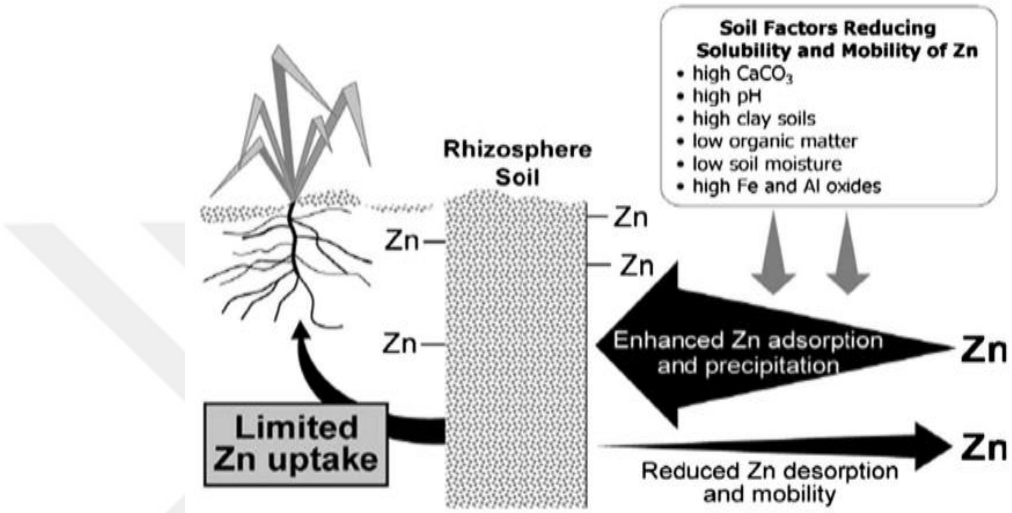

Figure 2.2. Soil factors contributing to low zinc bioavailability (Adapted from Gupta 2016)

To maintain zinc homeostasis, plants regulate a series of interconnected processes, including uptake, trafficking, storage, and detoxification. In soil, zinc predominantly exists in its divalent cation form (Zn^{2+}), which can bind to root-secreted organic compounds such as oxalate, malate, and citrate, facilitating its mobilization toward the roots (Suzuki et al. 2006). Notably, Zn^{2+} does not undergo oxidation or reduction. Plants absorb Zn^{2+} through their roots and transport it via xylem vessels to the shoots and leaves, ensuring its distribution throughout the plant.

2.5. Metal Transporters

Since zinc and other divalent transition metals (e.g., Fe, Cu, Mn, Cd, Ni) are hydrophilic and highly charged, they cannot passively diffuse across the cell membrane. Instead, their transport requires specific membrane-bound transporter proteins. The most prominent families of metal transporters include P-1B ATPases, natural resistance-associated macrophage proteins (NRAMPs), cation diffusion facilitators (CDFs), and zinc-regulated transporter/iron-regulated transporter-like proteins (ZIPs). To date, metal transporters have been identified using various approaches, including functional complementation of yeast mutants, sequence similarity analysis, database mining, hybridization, and polymerase chain reaction (PCR) (Guerinot 2000).

2.6. Zinc-Iron Regulated Transporter-like Protein (ZIP) Family

ZIPs represent one of the most essential families of metal transporters found across plants, animals, fungi, and bacteria, facilitating the influx of zinc from the extracellular environment into the cytosol. In most cases, the expression of ZIP genes encoding ZIP proteins is upregulated in response to zinc deficiency (Eide 1996). Structurally, most ZIP proteins consist of 309 to 476 amino acids and feature eight transmembrane domains spanning the N- and C-termini, although variants with seven or nine transmembrane domains have also been identified (Guerinot 2000). The metal-binding domain, rich in histidine residues, is located in a variable region between the third and fourth transmembrane domains, exhibiting limited sequence similarity among ZIP family members. The most conserved region of ZIP proteins is found within the fourth transmembrane domain.

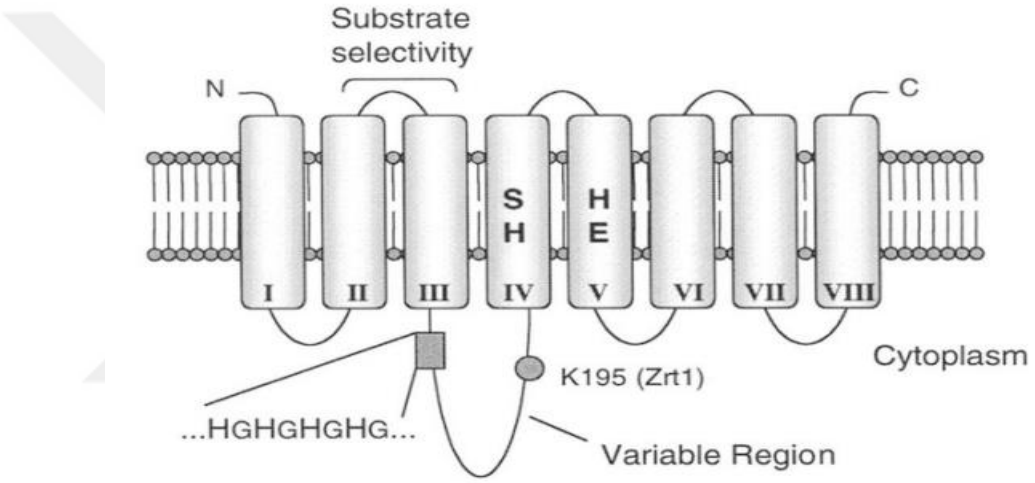

Figure 2.3. Predicted structural organization of ZIP proteins (Gaither 2001)

The majority of ZIP transporters are localized to the plasma membrane; however, some members are also found in intracellular compartments such as the endoplasmic reticulum (ER), vacuole, or chloroplasts (Krishna 2013).

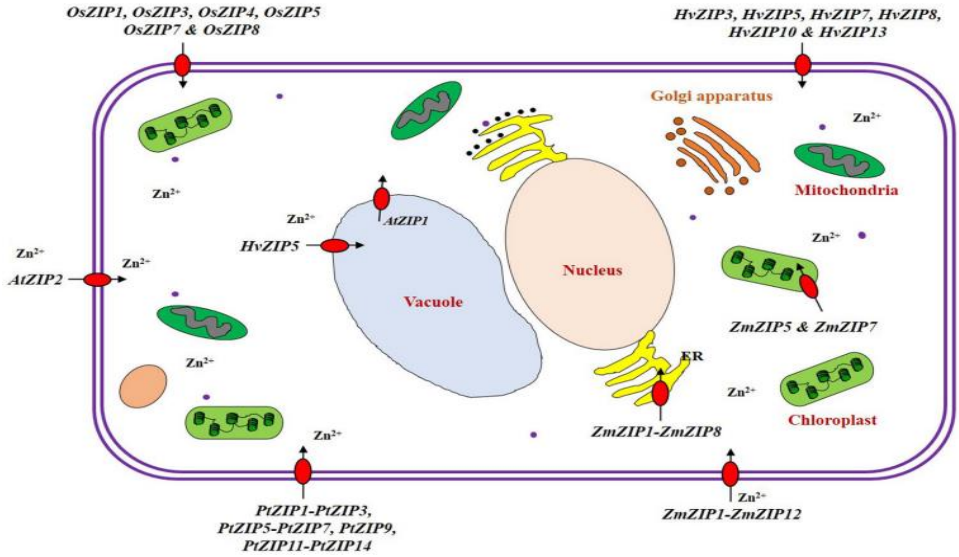

Figure 2.4. Cellular localization of ZIP transporter family across various crop species (Krishna 2016)

2.7. ZIP Genes Identified in Plants

The first ZIP genes in *Arabidopsis thaliana* were identified by Grotz et al. (1996), who demonstrated that *ZIP1* and *ZIP3* are upregulated in roots, while *ZIP4* is expressed in both shoots and roots under zinc-deficient conditions. Since then, more than 100 ZIP genes have been identified across various crop species, including wheat (Li et al. 2019; Durmaz et al. 2011), rice (Ramesh et al., 2013; Ishimaru et al. 2015), maize (Li et al. 2013; Mondal et al. 2013), barley (Tiong et al. 2015), *Medicago* (Lopez-Millán et al. 2004), lettuce (Gao et al. 2022), and grapevine (Cortés et al. 2012).

In rice (*Oryza sativa*), Lee et al. (2010) identified *OsZIP8* and demonstrated that its expression is induced under zinc-deficient conditions. Overexpression of *OsZIP8* resulted in decreased zinc accumulation in shoots and seeds, while increasing zinc content in roots. Similarly, Pedas et al. (2019) characterized ZIP transporters in barley (*Hordeum vulgare*), revealing that *HvZIP3* and *HvZIP8* function as low-affinity zinc transporters, whereas *HvZIP5* acts as a high-affinity transporter, as determined by yeast complementation assays.

2.8. Zinc Uptake in Yeasts

Zinc influx plays a crucial role in yeast physiology, as zinc is an essential trace element required for various cellular functions. In yeast, zinc uptake is mediated by the *ZRT1* and *ZRT2* genes, whose encoded transporters share 67% sequence similarity with each other (Eide et al. 1996). Yeasts possess two distinct zinc uptake systems: a high-affinity system, which is active under zinc-deficient conditions, and a low-affinity system, which operates when zinc levels are sufficient. *ZRT1* encodes the high-affinity zinc transporter, while *ZRT2* is responsible for the low-affinity system (Zhao and Eide 1996). Together, these two systems enable yeast to efficiently regulate intracellular zinc levels under varying environmental conditions. The expression of *ZRT1* and *ZRT2* is

regulated by *ZAP1*, a key transcription factor involved in zinc homeostasis. Notably, yeast strains with *zrt1 zrt2* double mutations require zinc concentrations that are 10^5-fold higher than those needed for wild-type growth, underscoring the importance of these transporters in zinc acquisition (Zhao and Eide 1996).

Due to their well-characterized zinc transport mechanisms, *zrt1 zrt2* double mutant yeast strains are commonly used in functional complementation assays, a method that was also employed in this study. This mutant lacks both high-affinity and low-affinity zinc uptake systems, making it highly sensitive to zinc limitation because it relies on less efficient zinc acquisition pathways.

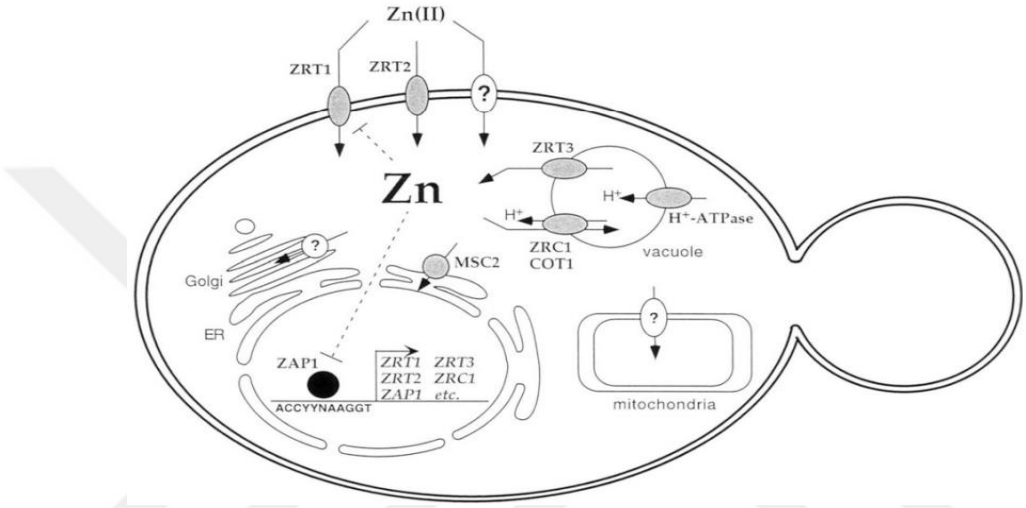

Figure 2.5. Model of ZRT1 and ZRT2 proteins involved in zinc transport in yeast (Gaither 2001)

2.9. Metal Chelators

Metal-chelating agents, commonly referred to as chelators, are compounds that form stable complexes with metal ions by creating ring-like structures known as ligands. This binding process reduces the ionic activity of metals, effectively altering their bioavailability (Kumar 2016). Chelating agents are widely used in functional complementation assays to facilitate the identification and characterization of target genes.

In the context of zinc deficiency studies, ethylenediaminetetraacetic acid (EDTA) and ethylene glycol-bis(β-aminoethyl ether)-N,N,N′,N′-tetraacetic acid (EGTA) are among the most frequently employed chelators. The primary distinction between EDTA and EGTA lies in their metal ion affinities: EDTA exhibits a strong affinity for zinc ions (Zn^{2+}), whereas EGTA preferentially binds to calcium ions (Ca^{2+}). Both agents are commonly used to induce zinc-deficient conditions by effectively sequestering free zinc ions.

3. MATERIALS AND METHODS

3.1. Vectors Used in the Study

The pAG426GPD-ccdB yeast expression vector (empty vector, EV) and the pAG426GPD vector containing the *PdZIP8* gene (pAG426GPD-PdZIP8) were already available in the Plant Transformation Laboratory of the Department of Agricultural Biotechnology at Akdeniz University.

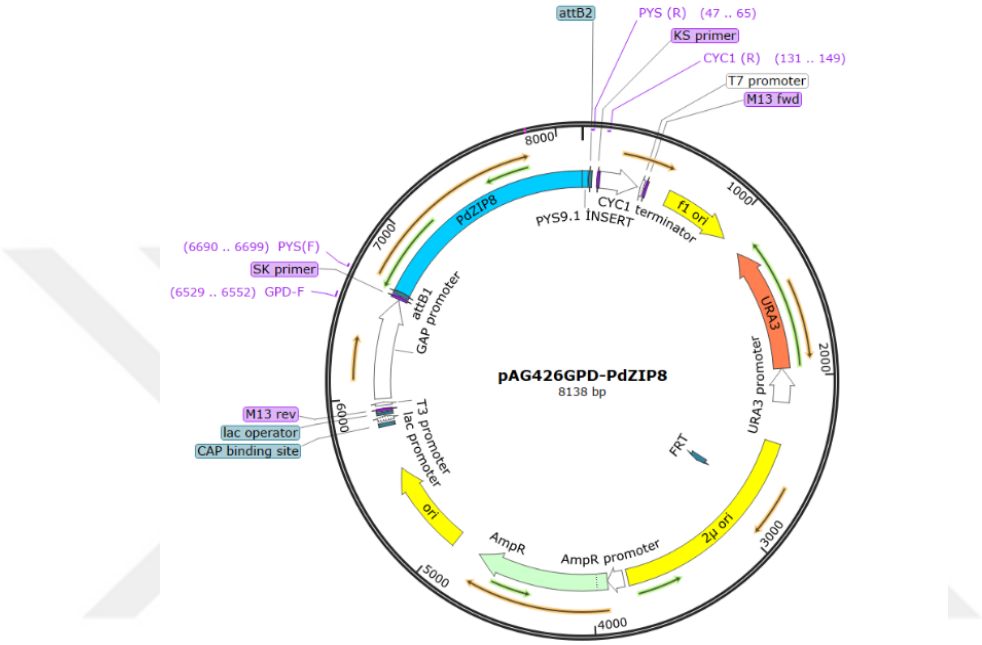

Figure 3.1. Map illustration of pAG426GPD-PdZIP8 (derived from Addgene plasmid #14156)

3.2. YPD (Yeast Extract Peptone Dextrose) and YNB (Yeast Nitrogen Base) Growth Media

YPD is a complete medium that contains yeast extract, peptone and dextrose, which are essential for optimal yeast growth. This medium is widely used for yeast cultivation. YNB is a medium that contains ammonium sulphate as its nitrogen source but lacks aminoacids. Therefore, it is used with CSM without uracil to facilitate the selection of yeast strains with specific auxotrophic requirements.

In the present study, YPD growth medium was used for the growth of yeast, while YNB growth medium was used to select for the yeast cells that harbor the desired plasmid.

3.3. Yeast Strains

The yeast (*S. cerevisiae*) strains used in this study were W303 and ZHY3. W303 is a derivative of the S288C strain, recognized as one of the first yeast strains to have its genome completely sequenced (Matheson et al. 2017). W303 is frequently used in research requiring auxotrophic markers, particularly in studies investigating mutations in genes involved in the biosynthesis of amino acids and nucleotides. Additionally, W303 is also known for its high transformation efficiency, enabling it to effectively uptake foreign DNA during genetic manipulation techniques such as transformation.

Yeast zinc uptake-responsible transporter genes are considered as *ZRT1* and *ZRT2*. ZHY3 yeast strain derived from W303 possesses mutations in both the *ZRT1* and *ZRT2* genes. As a result, it takes up only a minimal amount of zinc into the cell which is insufficient for proper growth. ZHY3 is widely used in yeast complementation assays to assess the zinc uptake abilities of candidate genes.

3.4. Transformation of Empty Vector (pAG426GPD) and pAG426GPD-PdZIP8 into W303 and ZHY3 Yeast Strains

The empty vector and the vector harboring the *PdZIP8* gene were transformed into the W303 and ZHY3 yeast strains following the LiAc/SS carrier yeast transformation method (Gietz 2006). W303 and ZHY3 yeast cells were streaked onto YPD agar plates and incubated at 30 °C for 3 days to allow colony formation. A single colony from each strain was selected using a sterile pipette tip and cultured in 5 ml of YPD liquid media at 30 °C in a shaker incubator set to 225 rpm overnight. The following day, the optical density (OD_{600}) was measured with a spectrophotometer, with an OD_{600} value of 0.1 corresponds to a concentration of $1x10^{6}$ cells/ml. The OD_{600} values obtained were 3.2 and 1.2 for W303 and ZHY3, respectively. The cells were subsequently diluted to an OD_{600} of 0.2 with 50 ml of 2X YPD liquid medium and incubated for approximately 5 hours at 30 °C in a shaker incubator at 225 rpm until the OD_{600} values reached 1.2. The carrier DNA was boiled in water for 5 min and then chilled immediately. The cells were centrifuged at 3.000 rpm for 5 min and the pellet was resuspended. Resuspended cells were centrifuged again at 3.000g for 5 min to suspend the cells and this washing procedure was repeated three times. The cells were then resuspended, and 100 µl of the cell suspension was centrifuged for transformation. Transformation components were added to each transformation tube, including a negative control, and the cells were resuspended by gentle flicking. The tubes were placed in a water bath at 42 °C and incubated for 40 min. After incubation, the tubes were centrifuged and the supernatant was discarded. The cell suspensions were spread onto YNB and YPD agar plates which were then incubated at 30 °C for 3 days for colony formation. After the incubation period, 6 colonies of ZHY3-PdZIP8 cells and 3 colonies of ZHY3-EV were selected. Each colony was resuspended in 20 µl of NaOH in a PCR tube. The tubes were incubated in a thermocycler (Biorad) at 95°C for 45 min. The cells were then spinned for 10 min and 1 µl of the supernatant was used as template. Colony PCR was performed using gene specific primers (ZIP8-F-ZIP8-R) as well as vector backbone primers (GPD-F-CYC1-R) as listed in Table 3.1 The PCR products were loaded onto a 1% agarose gel and subjected to electrophoresis at 80V for 40 mins.

Table 3.1. The sequence of primers used in colony PCR

Primer Name	Sequence
ZIP8-F	5′-GACTAGTCTCGCCGCGCA-3′
ZIP8-R	5′-ACGAGCTCACCACTTTGTACAAGAA-3′
GPD-F	5′-CGGTAGGTATTGATTGTAATTCTG-3′
CYC1-R	5′-GCGTGAATGTAAGCGTGAC-3′

Table 3.2. Colony PCR reaction components

Reaction Components	Volume
EcoTaq PCR Master Mix (2X)	8 µl
Forward Primer (ZIP8-F/ GPD-F)	1 µl
Reverse Primer (ZIP8-R/CYC-R)	1 µl
Template	1 µl
Nuclease-free H_2O	9 µl

Table 3.3. PCR conditions

Temperature	Time	Cycle
95°C	5 min	1
95°C	3 min	35
58°C	40 sec	
72°C	1.30 min	
72°C	7 min	1

3.5. Determination of the Deficient Zinc Concentrations of W303 and ZHY3 with EDTA and EGTA

Empty vector and pAG426GPD-PdZIP8 transformed W303 and ZHY3 yeast cells were streaked onto YNB growth media and incubated at 30 °C for 3 days for colony formation. Single colonies were then selected from the strains and suspended in 5 ml of YNB liquid media overnight. The following day, the OD_{600} values were measured and diluted to a concentration of 0.2. Ten-fold serial dilutions (OD_{600} values of 0.2, 0.02, 0.002, 0.0002) of these colonies were prepared and 5 µl of each dilution was spotted onto YNB media supplemented with varying concentrations of EGTA (0-25 mM) and EDTA (0-3200 µM). The cells were then incubated at 30°C for 3 days to assess the growth.

3.6. Zinc and Iron Uptake Assay in W303 and ZHY3 Yeast Cells

All glass and plastic materials used for ICP-MS analysis were sterilized by soaking in 10 % nitric acid. W303 and ZHY3 yeast cells transformed with either the empty vector or pAG426GPD-PdZIP8 construct were streaked onto YNB agar medium and incubated at 30 °C for 3 days. For each biological replicate, a single colony was selected and inoculated into 100 ml of liquid YNB medium, followed by incubation in a shaker at 30 °C for 24 hours. On the following day, cell density was determined by measuring the OD_{600} using a spectrophotometer. Cultures were then transferred into 300 ml of YNB medium supplemented with 5 µM EDTA to limit zinc and iron availability, with an initial OD_{600} adjusted to 0.2. Cells were grown for 48 hours under the same incubation conditions. After the incubation period, cultures were centrifuged at 6000 g for 5 minutes at 4 °C. The supernatants were discarded, and the resulting cell pellets were washed twice with cold ultrapure water. Subsequently, the pellets were incubated at 60 °C for 24 hours to determine dry weight. Dry weights were recorded, and the pellets were then digested by adding 6 ml of nitric acid (HNO_3), 1 ml of hydrochloric acid (HCl), and 2 ml of deionized water. After digestion, samples were filtered and the final volume was adjusted to 25 ml with ultrapure water. Prepared samples were submitted to LABEN analysis laboratory (Antalya) for ICP-MS analysis. For each construct, three independent biological replicates were analyzed.

3.7. Determination of the Subcellular Localization of PdZIP8 Protein

The *PdZIP8* gene fragment was designated for insertion into the yeast pAG426GPD-EGFP vector to generate a PdZIP8-EGFP fusion construct. The map illustration of PdZIP8-EGFP vector was given in figure 3.2.

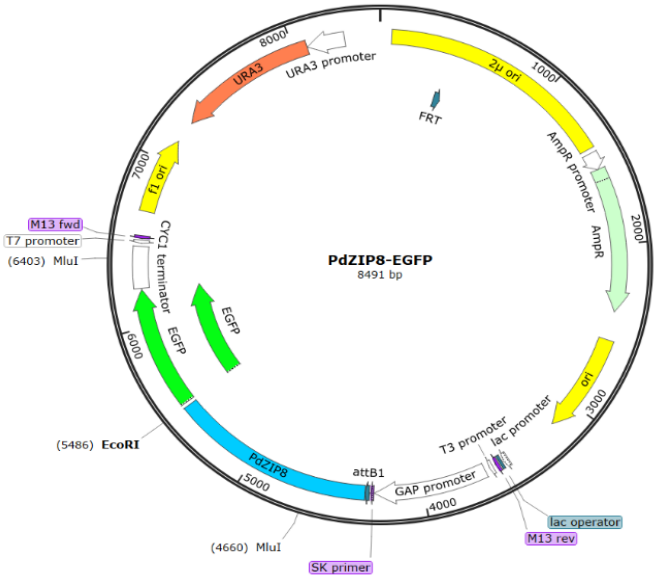

Figure 3.2. Map illustration of PdZIP8-EGFP vector (derived from Addgene plasmid #14204)

3.7.1. Designation of the Reverse Primer for the Amplification of *PdZIP8* gene

To construct the PdZIP8-EGFP fusion protein, the stop codon was removed from the selected reading frames of the *PdZIP8* gene, facilitating the integration of the GFP sequence. An appropriate restriction site (*EcoR*I) was added to the primer design. In selecting the restriction enzyme, careful consideration was given to maintaining the structural integrity of the GFP protein within the vector, ensuring that its fluorescence properties were preserved, while also avoiding frameshift mutations that could disrupt protein function. After designing the primer which includes 15-base complementary regions just before the stop codon, a 6-base restriction site and a 2-base linker region were added to the primer to facilitate enzymatic digestion and ligation processes.

3.7.2. Amplification of *PdZIP8* Gene Fragment

The vector backbone forward primer and the designed reverse primer including *EcoR*I restriction site were used to amplify the *PdZIP8* gene fragment. The PCR components detailed in Table 3.5 were used for the amplification. The PCR results and fragment sizes were visualized and confirmed through gel electrophoresis.

Table 3.4. The sequence of primers used in PCR

Primer Name	Sequence
GPD-F	5′-CGGTAGGTATTGATTGTAATTCTG-3′
EcoRI-PdZIP8-R	5′-CAGAATTCCACGCCCATTT-3′

Table 3.5. PCR reaction components

Reaction Components	Volume
EcoTaq PCR Master Mix (2X)	20 µl
GPD-F	2.5 µl
EcoRI-PdZIP8-R	2.5 µl
Template	2.5 µl
Nuclease-free H_2O	22.5 µl
Total	50 µl

Table 3.6. PCR conditions

Temperature	Time	Cycle
95°C	5 min	1
95°C	3 min	35
60°C	40 sec	
72°C	1.30 min	
72°C	7 min	1

3.7.3. Restriction Reaction of *PdZIP8* Gene Fragment and EGFP Vector

The *PdZIP8* PCR product and the EGFP vector were subjected to double digestion for cloning using the components specified in tables 3.7 and 3.8. A total of 2 µg of *PdZIP8* insert and 3 µg of EGFP vector was used separately for the reaction. The restriction mix was incubated at 37 °C for 1 hour to ensure complete enzymatic activity.

Table 3.7. Restriction reaction components for pAG426GPD-PdZIP8

Reaction Components	Volume
PdZIP8	7µl
*Eco*RI	1 µl
*Spe*I-HF	1 µl
Buffer (CutSmart)	5 µl
Nuclease-free H_2O	13 µl

Table 3.8. Restriction reaction components for pAG426GPD-EGFP

Reaction Components	Volume
pAG426GPD-EGFP	20 µl
*Eco*RI	1 µl
*Spe*I-HF	1 µl
Buffer (CutSmart)	5 µl
Nuclease-free H_2O	36 µl

The restricted plasmids were loaded onto a 0.8 % agarose gel and electrophoresis was conducted at 80 V for 1 hour. Expected bands were excised from the gel using a razor scapel, and subsequently eluted with the NEB Monarch® DNA Extraction Kit (NEB). The concentrations of purified products were quantified using the nanodrop device (Biodrop). The concentration of the insert DNA was measured at 30 ng/µl whereas the concentration of the vector was measured at 21 ng/µl.

3.7.4. Ligation Reaction

The *PdZIP8* gene fragments which had been digested from pAG426GPD-PdZIP8 were ligated to the pAG426GPD-EGFP using T4 DNA ligase, according to the manufacturer's instructions. A 1:3 vector insert ratio was used for the ligation reaction. The total reaction volume was adjusted to 20 µl and the following components were added in addition to the insert and vector: 1 µL of T4 ligase, 2 µL of ligase buffer, and 8 µl of nuclease-free H_2O. The samples were then placed in a PCR thermocycler at 4 °C overnight.

3.7.5. Transformation of the Ligated Vector to the *E. coli* Competent Cells

The PdZIP8-EGFP construct was transformed into *E. coli* DH5α competent cells following the heat shock method. Competent cells were taken out of the -80 ℃ glycerol stock and placed on ice until the cells were completely thawed. 50 µl of competent cells were used for the ligated product and another 50 µl competent cells were used as negative control. 5 microliters of plasmid were added to the 50 µl competent cells and mixed gently. The mixture was then placed on ice for 30 min, followed by a heat shock at 42 ℃ for 30 seconds. After heat shock, 900 µl of LB growth medium was added to each tube, and the tubes were incubated in a shaker incubator at 37 ℃ and 225 rpm for 1 hour. 150 µl of the cells were spread onto LB agar plates containing 100 µg/ml ampicillin. The plates were incubated overnight at 37 ℃.

3.7.6. Colony PCR

Colony PCR was performed to detect the *E. coli* colonies harboring the PdZIP8-EGFP plasmid. Three colonies were selected and transferred into tubes containing 500 µl of LB liquid medium. The cultures were incubated at 37 ℃ for 1 hour to allow for cell growth. 1 µl of the resulting mixture was added as the template to the PCR reaction, while this mixture was excluded from the negative control. The PCR was conducted according to Tables 3.5 and 3.6. The resulting PCR products were loaded onto a 1 % agarose gel, and gel electrophoresis was carried out at 80 V for 1 hour.

3.7.7. Plasmid Isolation from the Positive Colony

One of the positive colonies was selected and transferred into 5 ml of LB liquid medium containing 100 µg/ml ampicillin. The culture was incubated in a shaker at 37 ℃ overnight to facilitate growth. The following day, plasmid isolation was conducted using GeneJET Plasmid Miniprep Kit (Thermo Fisher, USA) according to the manufacturer's instructions.

3.7.8. Plasmid Restriction Reaction

The restriction reaction was conducted to assess the integration of the insert into the plasmid and to confirm the correct ligation and integrity of the construct. The PdZIP8-EGFP and pAG426GPD-EGFP vectors were subjected to restriction digestion using the reaction components outlined in Table 3.9 at 37 ℃ for 1 hour. 1 µg of PdZIP8-EGFP and 1 µg of EGFP plasmids were used separately for the reaction. The restricted products were then visualized on a 1 % agarose gel.

Table 3.9. Restriction reaction components

Reaction Components	Volume
PdZIP8-EGFP/ pAG426GPD-EGFP	10 µl
Buffer (3.1)	5 µl
*Mlu*I	2 µl
Nuclease-free H_2O	33 µl
Total	50 µl

3.7.9. Transformation of PdZIP8-EGFP and pAG426-EGFP vectors to ZHY3 yeast cells

The vectors were transformed into ZHY3 yeast cells using the method described in section 3.4. Colonies emerged after a 3-day incubation period after transformation. ZHY3-EGFP was used as a positive control while ZHY3-EV served as a negative control. One colony from each was selected and added to falcon tubes containing 5 ml of YNB liquid media. The tubes were placed in a 30 °C shaker incubator at 225 rpm overnight. A 3 % agarose pad was prepared and 40 µl of the pad was added to each microscope slide to immobilize the cells. Ten microliters of ZHY3 yeast cells were added to the agarose pads, and the slides were covered with microscope cover slides. Initial observations were conducted under the light microscope (Leica). Fluoresence was detected in PdZIP8-EGFP and pAG426GPD-EGFP vector containing ZHY3 cells. However, no floresence right was detected on ZHY3-EV cells. Further analysis was performed in ESOGÜ, Central Research Laboratory and Application Center, using ZEISS LSM800 laser confocal microscope (Carl Zeiss Microscopy) to determine the precise cellular localization of the PdZIP8 protein within ZHY3 cells.

3.8. Determination of the Zinc Uptake of *PdZIP8* in *Arabidopsis thaliana*

3.8.1. Arabidopsis Growth Conditions and Selection of the Homozygous Lines

The Arabidopsis genotypes used in this study were the wild-type (WT) accession Columbia (Col-0) and six Col-0 lines harboring *PdZIP8* transgenes, which were already available in our laboratory. The T1 lines were classified as PdZIP8-3, PdZIP8-7, PdZIP8-8, PdZIP8-10, PdZIP8-11 and PdZIP8-12. 100 seeds of each T1 transgenic lines were selected. Selected seeds were surface-sterilized with 70 % ethanol (EtOH) and 50 % sodium hypochlorite (NaCIO) and placed on petri dishes containing Murashige and Skoog (MS) growth media with 25 µg/ ml hygromycin to determine the segregation ratio. After vernalization for 2 days at 4 °C in darkness, the plates were transferred to a growth chamber. Seedlings were grown at 22 °C under a 16 hour light/8 hour dark photoperiod. After 13 days, five hygromycin-resistant arabidopsis plantlets of each line was chosen, and acclimatized on soil pots. This procedure was repeated until

the lines reached the T3 generation and displayed homozygous segregation. 3 lines (7-1, 11-2 and 12-3 were selected based on their hygromycin resistance ability and homozygosity.

Figure 3.3. Arabidopsis seed sterilization process

3.8.2. Confirmation of the Presence of the *PdZIP8* Gene via PCR

DNA from the selected lines (7-1, 11-2, and 12-3) was isolated following the CTAB-mediated DNA isolation protocol (Doyle 1991). DNA from WT lines was also isolated and used as a negative control. Fresh plantlets were harvested and placed into 1.5 ml microcentrifuge tubes. A volume of 150 µl of CTAB solution was added to each tube. The leaves were thoroughly ground using a pestle. An additional 300 µl of CTAB solution was then added, and the tubes were tightly closed and incubated in a 65 °C water bath for 2 hours. Following incubation, 450 µl of chloroform: isoamyl alcohol solution (24:1) was added to each tube. The tubes were centrifuged at 13.000 rpm for 20 minutes. The supernatants obtained after centrifugation were transferred to new microcentrifuge tubes. An equal volume of chloroform: isoamyl alcohol solution (24:1) was added to the supernatants. The mixtures were centrifuged again at 13.000 rpm for 20 minutes.

The upper aqueous phases were transferred to new tubes, and an equal volume of cold isopropyl alcohol was added. The tubes were gently inverted 4–6 times to ensure thorough mixing. Samples were incubated at -20 °C for 1 hour and subsequently centrifuged at 13.000 rpm for 20 minutes. Without disturbing the pellets formed at the bottom of the tubes, the supernatants were carefully removed using a pipette. To wash the pellets, 300 µl of 70 % ethanol (pre-cooled to -20 °C) was added to each tube, followed by centrifugation at 13.000 rpm for 20 minutes. The supernatants were

removed again, and this ethanol wash step was repeated once more. After the final centrifugation, the remaining ethanol was carefully removed without damaging the pellets, which were then left to air-dry at room temperature. After ethanol evaporation, each pellet was resuspended in 50 µl of nuclease-free water. PCR reaction was set using isolated DNA of the WT, 7-1, 11-2, 12-3 lines as templates. Gene specific PdZIP8-F and PdZIP8-R primers were used as given in Table 3.2. The PCR components and conditions were listed in Tables 3.3 and 3.4 The PCR samples were then run on a 1 % agarose gel and visualized.

3.8.3. Real Time Quantitative PCR (RT-qPCR) Analysis of *PdZIP8* Overexpressing Arabidopsis Lines

To evaluate the *PdZIP8* gene expression under standard condition, RT-qPCR analysis was performed. The seeds of WT and transgenic lines 7-1, 11-2, 12-3 were surface sterilized and sown on MS agar media. The seeds were vernalized for 2 days at 4 °C in darkness, the plates were transferred to a growth chamber. Seedlings were grown at 22 °C under a 16 hour light/8 hour dark photoperiod. After 13 days, plant materials were collected and total RNA was isolated from each using RNA Plant Mini Kit (Qiagen) according to manufacturer's instructions. Each RNA samples were run on a 1 % agarose gel using the electrophoresis method. Turbo DNase (Promega) was applied to each RNA sample to clean DNA impurities. The RNA samples were again run on a 1 % agarose gel and visualized. The concentration of the RNA samples were then measured on Qubit Fluorometric Quantification device (Invitrogen).

RT-qPCR analysis was performed using the device (BioRad). The expression of the *PdZIP8* gene was calculated using 10 ng of RNA treated with DNase and the Luna® Universal One-Step RT-qPCR Kit (NEB). The primers used are listed in Table 3.10 and the reaction was set up as described in Table 3.11. Samples were run in triplicate and normalized to *PDF2*. Relative gene expression levels were calculated using the ΔCt method (Livak and Schmittgen 2001). Since Col-0 lacks the transgene and served as a negative control, a very low or undetectable signal for *PdZIP8* was expected. Therefore, -ΔCt values were used for visualizing and comparing expression levels.

Table 3.10. The sequence of primers used in RT-qPCR

Primer Name	Sequence
PdZIP8Q-F	5′-GATCCGGACACCATCAGACC-3′
PdZIP8Q-R	5′-GATATACCCCAGCCGACGAG-3′
PDF2Q-F	5′-TCATTCCGATAGTCGACCAAG-3′
PDF2Q-R	5′-TTGATTTGCGAAATACCGAAC-3′

Table 3.11. RT-qPCR reaction components

Reaction Components	Volume
Luna Universal One-Step Reaction Mix (2X)	2.5 µl
Luna WarmStart® RT Enzyme Mix (20X)	0,25 µl
Forward primer (10 µM)	0.4 µl
Reverse primer (10 µM)	0.4 µl
Template RNA	2 µl
Nuclease-free H_2O	4.45 µl
Total	10 µl

3.8.4. Phenotypic Characterization of WT and PdZIP8-Overexpressing Arabidopsis Lines

For phenotypic characterization, seeds of WT and transgenic Arabidopsis lines were surface sterilized and sown on petri plates containing five differently modified MS media: (1) MS supplemented with 30 µM $ZnSO_4$ and 100 µM $FeSO_4$, (2) MS with 15 µM $ZnSO_4$ and 100 µM $FeSO_4$, (3) MS with 0 µM $ZnSO_4$ and 100 µM $FeSO_4$ (4) MS with 30 µM $ZnSO_4$ and 0 µM $FeSO_4$, and (5) MS with 0 µM $ZnSO_4$ and 0 µM $FeSO_4$. After vernalization for 2 days at 4 °C in darkness, the plates were transferred to a growth chamber. Seedlings were grown at 22 °C under a 16-hour light/8-hour dark photoperiod. Root and leaf lengths of 10 seedlings from each line were measured after 13 days using the ImageJ software program.

3.8.5. Metal Element Analysis and Measurements of the Fresh and Dry Weights of WT and *PdZIP8* Overexpressing Arabidopsis Lines

For fresh and dry weight measurements, seeds of WT and transgenic Arabidopsis lines were surface-sterilized and sown in Magenta boxes containing Murashige and Skoog (MS) media modified with different zinc and iron concentrations. Five media compositions were used: (1) MS supplemented with 30 µM $ZnSO_4$ and 100 µM $FeSO_4$ (2) MS with 10 µM $ZnSO_4$ and 100 µM $FeSO_4$, (3) MS with 0 µM $ZnSO_4$ and 100 µM $FeSO_4$, (4) MS with 30 µM $ZnSO_4$ and 0 µM $FeSO_4$, and (5) MS with 0 µM $ZnSO_4$ and 0 µM $FeSO_4$. After stratification at 4 °C in darkness for 2 days, the boxes were transferred to a growth chamber and maintained at 22 °C under a 16-hour light/8-hour dark photoperiod for 1 month. At harvest, 15 fresh plants per line were collected and weighed, with three biological replicates per line per condition. The same samples were then dried in an incubator at 70 °C for 2 days and reweighed to determine dry biomass.

For metal element analysis by ICP-MS, a separate set of seeds (400 per line) was surface-sterilized and sown in Magenta boxes containing MS media with either 10 µM $ZnSO_4$ (zinc-deficient condition) or 30 µM $ZnSO_4$ (zinc-sufficient condition), both supplemented with 100 µM $FeSO_4$. After a 2-day stratification at 4 °C in darkness, seedlings were grown under identical growth conditions as described above for 1 month. Following growth, plant tissues were harvested, dried at 70 °C for 2 days, and sent to the LABEN Analysis Laboratory (Antalya, Turkey) for inductively coupled plasma mass spectrometry (ICP-MS) analysis.

3.8.6. Measurements of Chlorophyll Concentrations in WT and *PdZIP8*-Overexpressing Arabidopsis Lines

0.25 grams of each line in each condition given in section 3.8.5 were harvested and chlorophyll was extracted with 10 ml of 80 % acetone. After homogenization, the samples were incubated for 15 min on the ice, and then centrifuged at 15.000 g for 10 min, the supernatant was diluted and taken to measure A663 and A643 with a spectrophotometer. Total chlorophyll contents, including Chl a and b, were determined according to the method of Arnon (Arnon 1949). Three biological replicates were used for measurements of chlorophyll concentrations.

4. FINDINGS

4.1. Transformation of Empty Vector (EV) (pAG426GPD) and pAG426GPD-PdZIP8 into W303 and ZHY3 Yeast Strains

Following a three-day incubation at 30°C, transformant colonies were observed, confirming successful transformation. In contrast, no colony formation was detected in the negative control group, where cells lacked the plasmid. These results demonstrate the effectiveness of the transformation process.

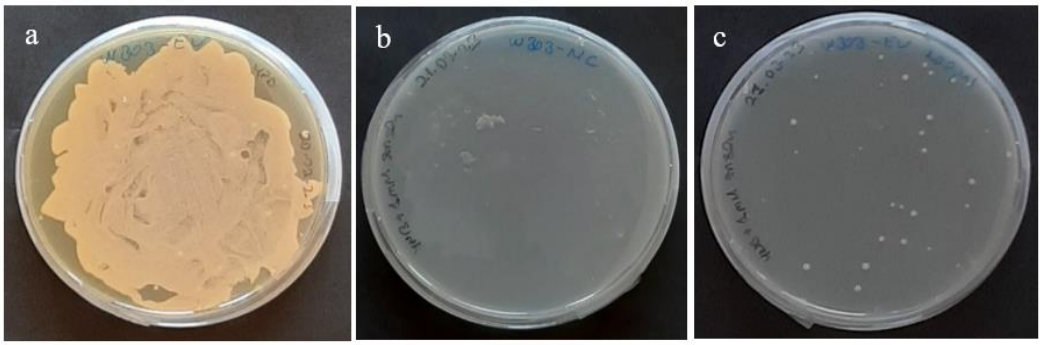

Figure 4.1. Transformation of empty vector (EV) (pAG426GPD) into W303 yeast strain; **a)** W303-EV on YPD medium (positive control); **b)** W303 cells spreaded on YNB medium (negative control); **c)** Transformed W303-EV cells spreaded on YNB medium

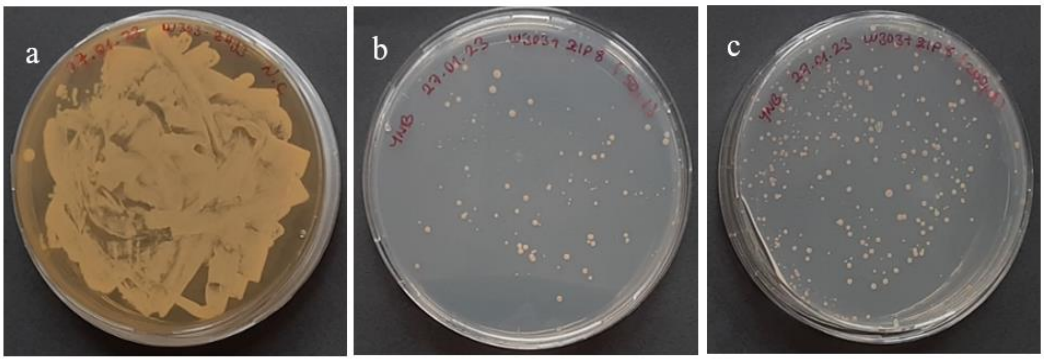

Figure 4.2. Transformation of pAG426GPD-PdZIP8 into W303 yeast strain; **a)** W303-PdZIP8 cells spreaded on YPD medium (positive control); **b, c**) W303-PdZIP8 cells spreaded on YNB media

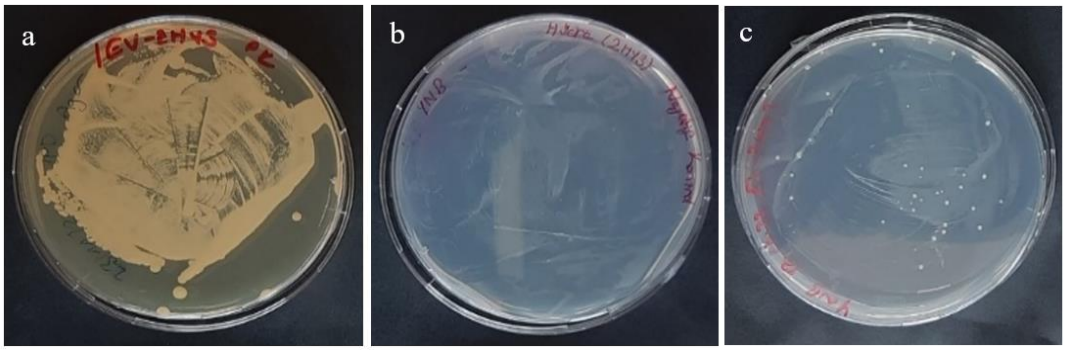

Figure 4.3. Transformation of empty vector (EV) (pAG426GPD) to ZHY3 yeast strain; **a)** ZHY3-EV spreaded on YPD medium (positive control); **b)** ZHY3 cells spreaded on YNB medium (negative control); **c)** Transformed ZHY3-EV cells spreaded on YNB medium

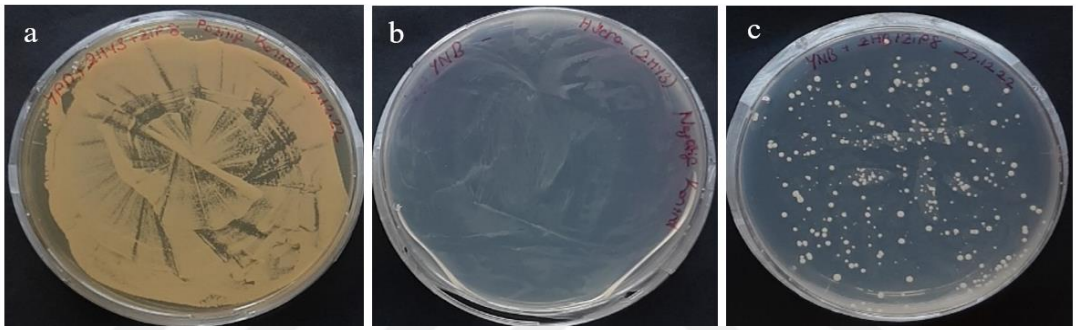

Figure 4.4. Transformation of pAG426GPD-PdZIP8 to ZHY3 yeast strain; **a)** ZHY3-PdZIP8 spreaded on YPD medium (positive control); **b)** ZHY3 cells spreaded on YNB medium (negative control); **c)** Transformed ZHY3-PdZIP8 cells spreaded on YNB medium

4.2. Colony PCR from ZHY3-EV and ZHY3-PdZIP8 cells

Three colonies of ZHY3-PdZIP8 were selected, and colony PCR was performed using vector backbone primers (GPD-F and CYC-R) to confirm the presence of the pAG426-PdZIP8 construct. The expected band size was 1759 bp. One of the colonies showed the expected band, indicating successful transformation of the vector into that ZHY3 colony.

To further confirm the presence of the *PdZIP8* gene in the construct, colony PCR was performed on another three colonies using gene-specific primers (ZIP8-F and ZIP8-R). The expected band size for this reaction was 1514 bp, and all three colonies produced the expected band, confirming the presence of the *PdZIP8* gene in these ZHY3 colonies.

Additionally, colony PCR was performed on ZHY3-EV colonies using the same vector backbone primers (GPD-F and CYC-R) to verify the presence of the empty vector (EV). The expected band size was 1908 bp, and two out of three colonies showed the expected band, confirming successful transformation of the EV into those ZHY3 cells.

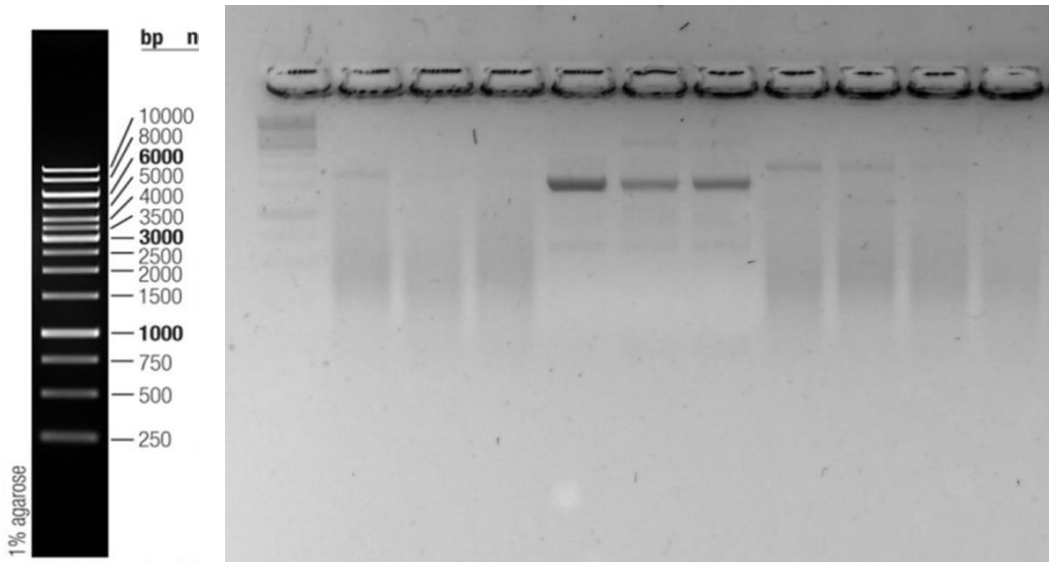

Figure 4.5. Colony PCR results; **1-3)** ZHY3-PdZIP8 (confirmed with vector-backbone primers- 1759 bp); **4-6)** ZHY3-PdZIP8 (confirmed with gene-specific primers-1514 bp); 7-9) ZHY3-EV (confirmed with vector-backbone primers-1908 bp); **10)** negative control

4.3. Determination of the Zinc Deficient Concentrations of W303 and ZHY3 with EDTA and EGTA

To create zinc deficient conditions, two types of chelators were added to the YNB growth media at varying concentrations. Cells were spotted onto YNB plates in 10-fold serial dilutions, as shown above the plates, with chelator concentrations indicated below each plate.

For EGTA, the zinc deficient concentration was determined to be 25 mM for both W303-EV and W303-PdZIP8 cells. No significant growth differences were observed between W303 cells harboring the plasmid with or without the *PdZIP8* gene. However, a significant difference in growth was observed between ZHY3-EV and ZHY3-PdZIP8 cells. ZHY3-EV cells were unable to grow above YNB medium containing 12.5 mM EDTA, as this cell type is a zinc uptake mutant. In contrast, ZHY3-*PdZIP8* effectively complemented the zinc deficiency in the growth media and exhibited growth up to 20 mM of EGTA. These findings indicate that *PdZIP8* successfully complements the zinc uptake deficiency in ZHY3 cells, enabling growth under zinc-deficient conditions induced by EGTA. This suggests that *PdZIP8* functions as a zinc transporter in the zinc uptake-deficient yeast.

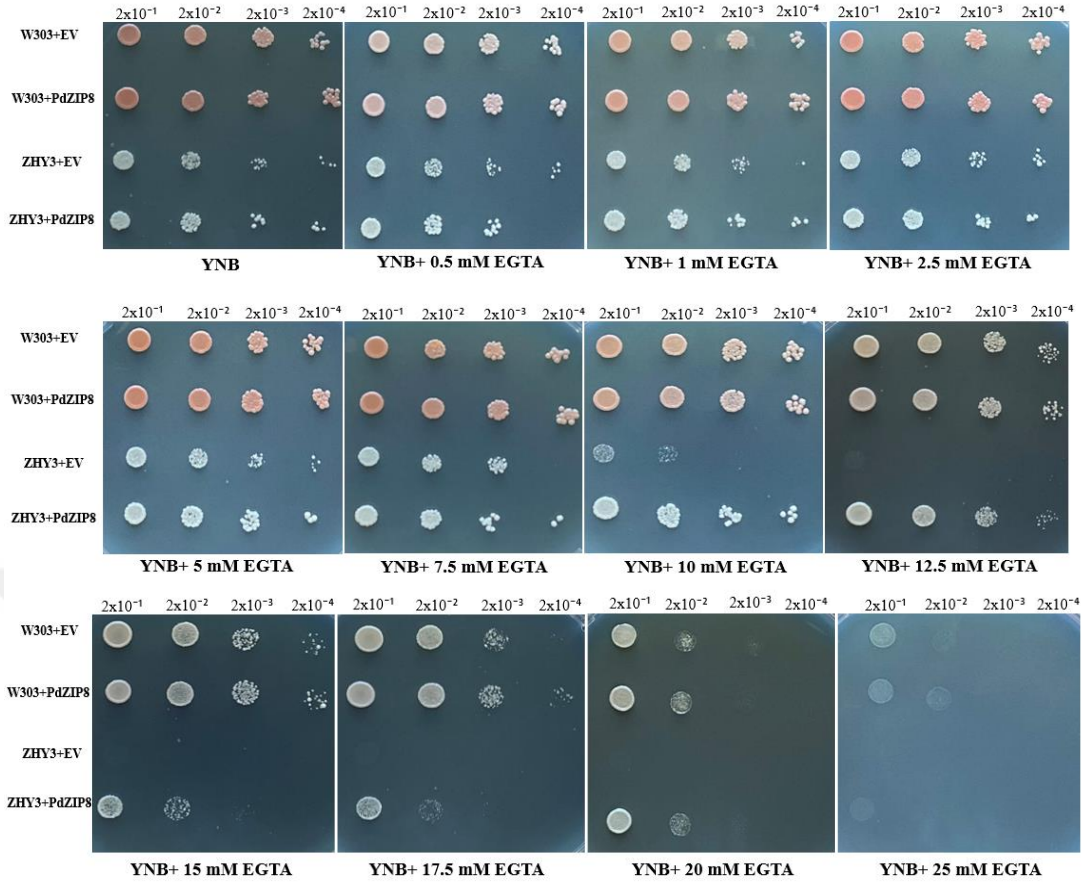

Figure 4.6. Determination of the zinc deficient concentrations of W303 and ZHY3 with EGTA

For EDTA, the zinc-deficient concentration was determined to be 1600 µM for both W303-EV and W303-PdZIP8 cells. No significant growth differences were observed between W303 cells harboring the plasmid with or without the *PdZIP8* gene. However, a significant difference in growth was observed between ZHY3-EV and ZHY3-PdZIP8 cells. ZHY3-EV cells were unable to grow above YNB medium containing 10 µM EDTA, as this strain is a zinc uptake mutant. In contrast, ZHY3-PdZIP8 effectively complemented the zinc deficiency in the growth media and exhibited growth up to 200 µM EDTA. Notably, this concentration represents a nearly 20-fold increase in zinc deficiency, yet *PdZIP8* was still able to restore zinc uptake and support robust yeast growth, while EV-containing cells failed to grow and died under these conditions.

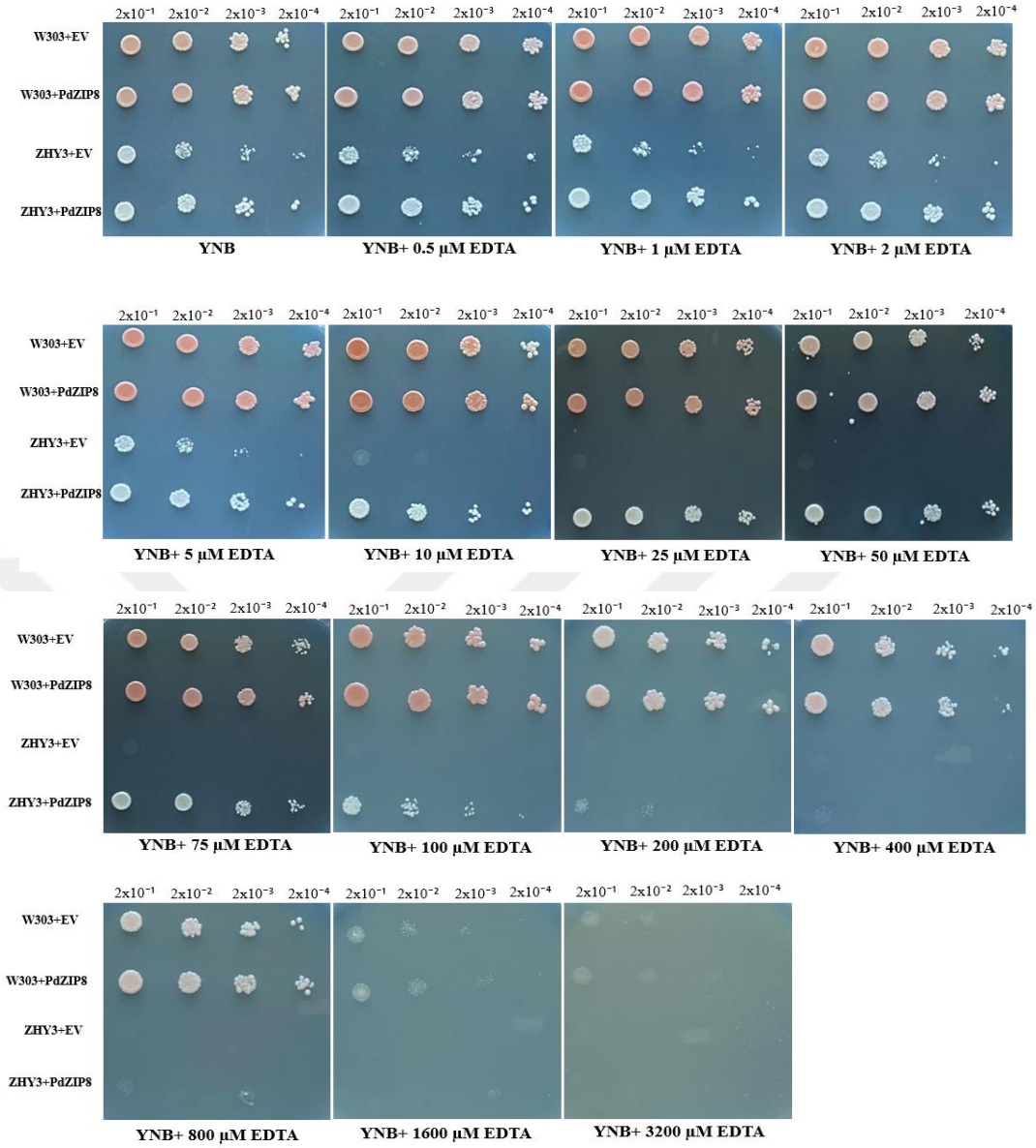

Figure 4.7. Determination of the zinc deficient concentrations of W303 and ZHY3 with EGTA

4.4. Zinc and Iron Uptake Assay in W303 and ZHY3 Yeast Cells

ICP-MS analysis showed that metal accumulation varied between yeast strains and constructs. The highest zinc and iron concentrations were found in W303-PdZIP8 cells, with average values of 57.7 µg/mg zinc and 13.6 µg/mg iron. W303-EV cells had the second-highest levels, averaging 40.3 µg/mg zinc and 11.4 µg/mg iron. This shows that the W303 wild-type strain, which already contains functional zinc transporter genes, supports higher metal uptake.

In contrast, the ZHY3 strain is a mutant lacking key zinc uptake genes. In this background, *PdZIP8* expression significantly increased zinc and iron accumulation. ZHY3-PdZIP8 cells accumulated 30.6 µg/mg zinc and 8.8 µg/mg iron, whereas ZHY3-EV controls showed the lowest values, with 7.9 µg/mg zinc and 6.4 µg/mg iron. These

results indicate that *PdZIP8* complements the zinc uptake defect in ZHY3 and enhances metal accumulation. Overall, zinc uptake appeared to be more pronounced than iron uptake across all samples, highlighting the zinc transport capability of *PdZIP8*.

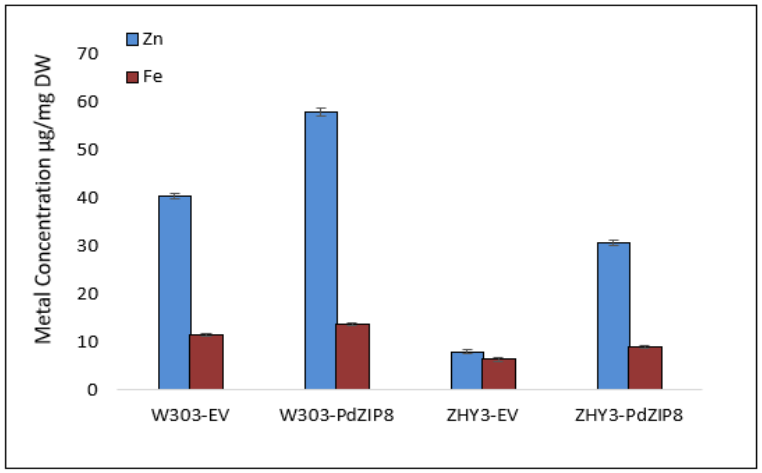

Figure 4.8. Zinc and iron concentrations of W303 and ZHY3 yeast strains containing *PdZIP8* gene and empty vector

4.5. Determination of the Subcellular Localization of PdZIP8 Protein

4.5.1. Amplification of the Targeted *PdZIP8* gene

A 50 µl of PCR reaction was prepared according to Tables 3.5 and 3.6. The *PdZIP8* gene was amplified using the primers GPD-F and EcoRI-R, with an expected band size of 1324 bp. A sample without template was included as a negative control, and a 1 kb ladder was used for size reference.

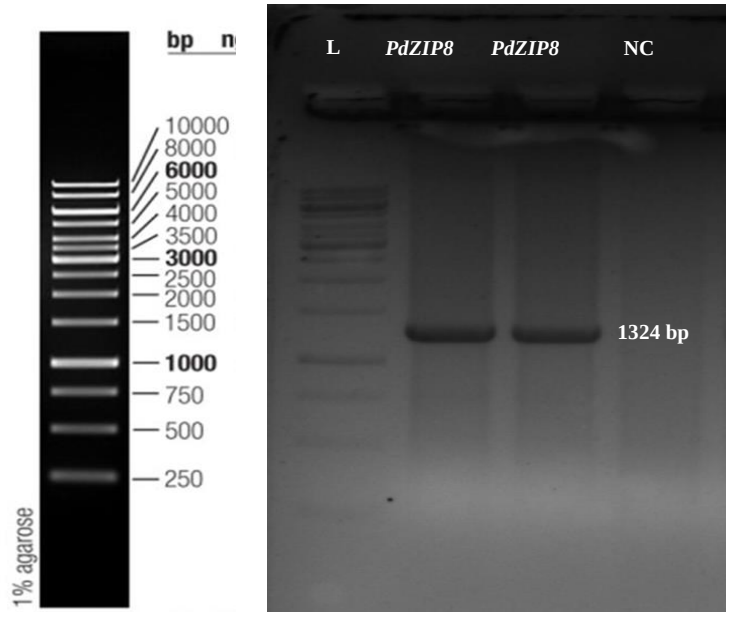

Figure 4.9. PCR bands of amplified *PdZIP8* gene fragment with GPD-F and EcoRI-R primers

4.5.2. Restriction Reaction of PdZIP8 Gene Fragment and pAG426GPD-EGFP Vector

Prior to ligation, the amplified *PdZIP8* fragment and the pAG426GPD-EGFP vector were digested with *Spe*I-HF and *Eco*RI. The expected sizes were 1324 bp for the uncut *PdZIP8* PCR product, 1200 bp for the digested *PdZIP8*, 9031 bp for uncut pAG426GPD-EGFP vector and 6571 bp, 1271 bp, and 464 bp for the digested pAG426GPD-EGFP vector.

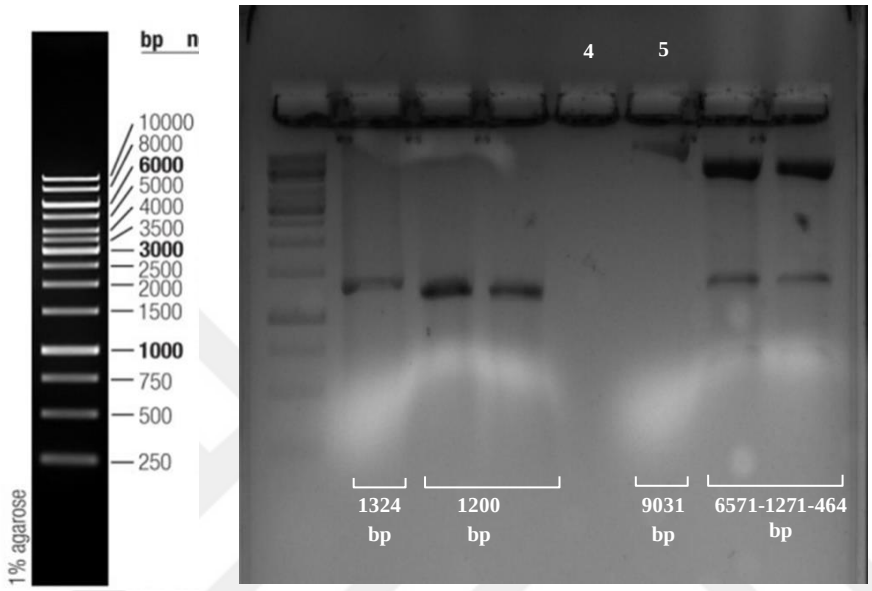

Figure 4.10. Restriction reaction of *PdZIP8* gene fragment and pAG426GPD-EGFP vector; **1)** uncut *PdZIP8* PCR product **2-3)** digested *PdZIP8* fragment; **5)** uncut pAG426GPD-EGFP vector; **6-7)** digested pAG426GPD-EGFP vector

4.5.3. Transformation of the Ligated Vector to the *E. coli* Competent Cells

The *PdZIP8* gene ligated to the EGFP vector was transformed into the *E. coli* DH5α competent cells. The vector without the inserted *PdZIP8* gene was used as a negative control. The transformed cells were spreaded onto LB agar plates, both with or without 100 µg/ml ampicillin. Colonies were formed on the plates containing PdZIP8-EGFP vector. However, no colony formation was observed for the negative control, since the ccdB gene was present on non-ligated GFP vector which causes toxicity and death of the cells. These results suggest that transformation was successful.

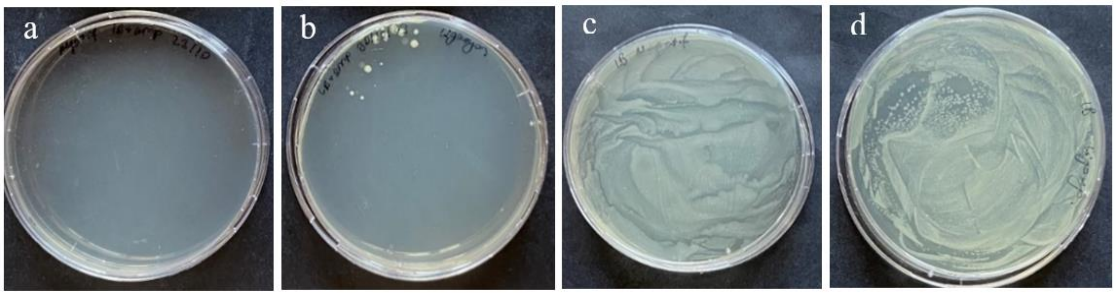

Figure 4.11. Transformed *E. coli* cells; **a)** Cells carrying GFP vector without the inserted *PdZIP8* gene spreaded on LB medium containing ampicillin as a negative control; **b)** Colonies carrying the ligated *PdZIP8* gene to GFP vector spreaded onto LB medium containing ampicillin; **c)** Cells carrying GFP vector without *PdZIP8* gene inserted spreaded onto LB medium; **d)** Colonies carrying the ligated *PdZIP8* gene to GFP vector spreaded onto LB medium

4.5.4. Colony PCR of Positive Transformants

Two colonies were selected from the LB agar plate containing ampicillin (Figure 4.10, plate b) and mixed with 500 µl of LB liquid medium. The mixtures were placed in a shaker incubator at 37 °C and 250 rpm. One microliter of each cell mixture was used for PCR. One microliter of LB liquid medium was used as negative control. The components listed in Table 3.5 were used and the PCR conditions were set according to the Table 3.6. The resulting PCR products were loaded on 1% agarose gel, subjected to electrophoresis at 80 V for 1 hour and visualized. The PCR result showed that colony one carried the expected 1990 bp band; therefore, it was selected for plasmid isolation step, as the presence of the correct band size confirmed the successful insertion of the target gene into the plasmid.

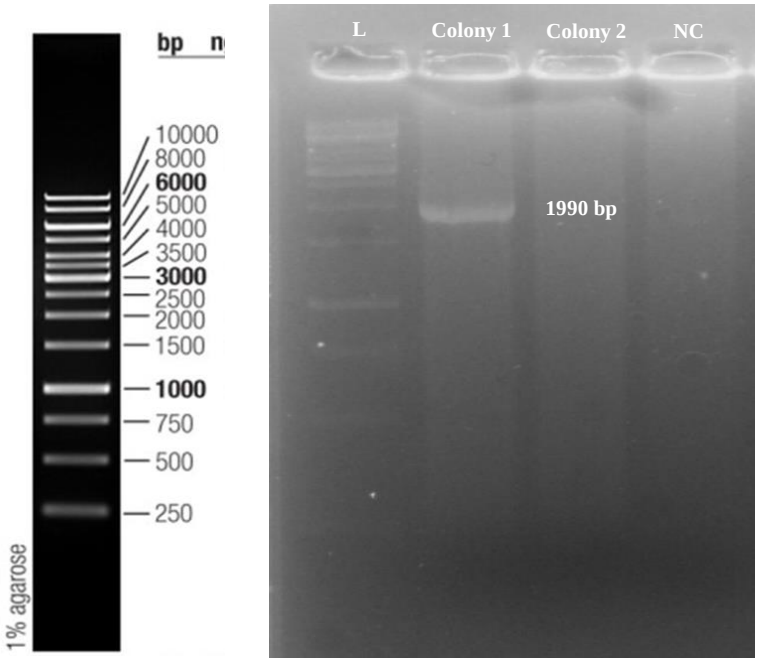

Figure 4.12. Colony PCR result of positive transformants

4.5.5. Plasmid Restriction Reaction

Plasmids containing the *PdZIP8* gene and empty vectors were isolated from the selected colonies using the method described in Section 3.7.8. Their concentrations were measured using a NanoDrop device (BioDrop), and both samples yielded 100 ng/µl. Restriction digestion was carried out using the components listed in Table 3.9. The resulting DNA fragments were separated on a 1% agarose gel by electrophoresis at 80 V for 1 hour. The expected fragment sizes were 8491 bp for the uncut PdZIP8-EGFP plasmid, 1743 bp and 6748 bp for the digested PdZIP8-EGFP construct, and 6943 bp for the digested EGFP vector. The results clearly showed that, under identical restriction enzyme conditions (*Mlu*I), the fragment sizes differed between the PdZIP8-EGFP and EGFP vectors. The observed fragment pattern matched the expected sizes, confirming the successful integration of the *PdZIP8* gene. This analysis was conducted to verify the accuracy of the cloning process and ensure that the target gene was correctly inserted into EGFP vector.

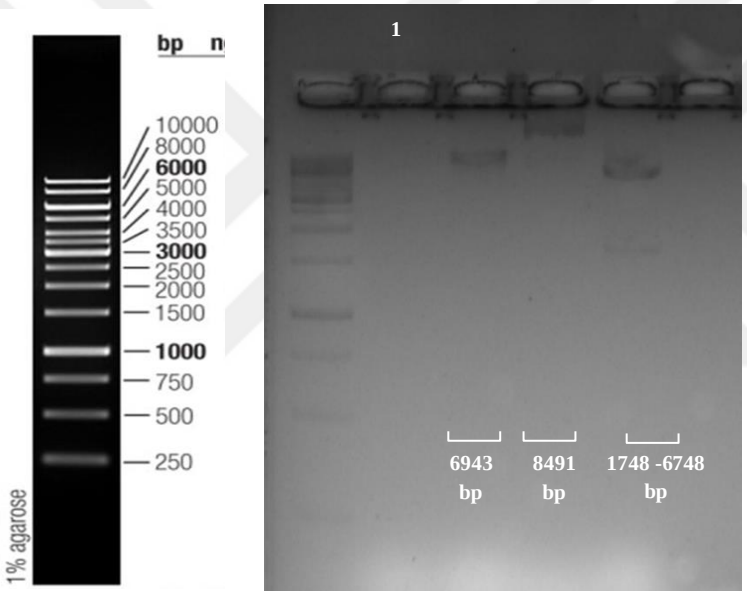

Figure 4.13. Confirmation of the plasmid construct by restriction reaction; **2)** digested EGFP vector**; 3)** uncut PdZIP8-EGFP vector; **4)** digested PdZIP8-EGFP vector

4.5.6. Transformation of PdZIP8-EGFP and EGFP Vectors to ZHY3 Yeast Strain

The vectors were transformed into the zinc uptake genes mutant yeast strain ZHY3 following the protocol outlined on section 3.4. Colony formation was observed in ZHY3 cells carrying PdZIP8-EGFP vector. pAG426GPD-EGFP vector was transformed as a positive control whereas cells without any vector transformed served as a negative control. Colonies were formed after 3 days of incubation time, indicating that the transformation into the ZHY3 was successful.

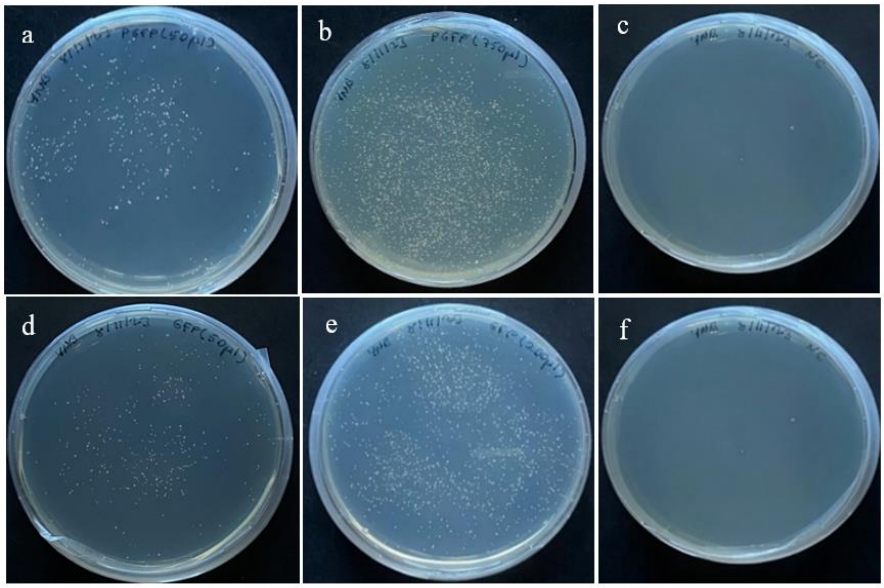

Figure 4.14. Transformation of PdZIP8-GFP and pAG426GPD-EGFP vectors into ZHY3; **a-b)** PdZIP8-GFP transformed cells on YNB; **c-f)** negative control; **d-e)** pAG426GPD-EGFP vector transformed cells on YNB (positive control)

4.5.7. Confocal Microscopy Images

pAG426GPD-ccdB (EV), pAG426GPD-EGFP (EGFP) and PdZIP8-EGFP vectors were transformed into ZHY3 yeast cells, and the cells were visualized using confocal microscopy to assess the expression and localization of GFP-tagged proteins. As expected, no fluorescence signal was detected in ZHY3 cells including EV, which lack the GFP gene in their plasmid construct. In contrast, strong GFP fluorescence was observed in both EGFP and PdZIP8-EGFP transformed ZHY3 cells. In EGFP transformed ZHY3 cells, the GFP signal was uniformly distributed throughout the cytosol, consistent with the expression of free GFP. However, in PdZIP8-EGFP transformed cells, the fluorescence localized predominantly to the plasma membrane and endoplasmic reticulum (ER), indicating targeted localization of the PdZIP8-GFP fusion protein. These localization patterns suggest that PdZIP8 may be an integral membrane protein with roles associated with membrane-bound compartments. Its presence in the ER, in particular, raises the possibility that PdZIP8 is involved in processes such as protein folding, quality control, or trafficking.

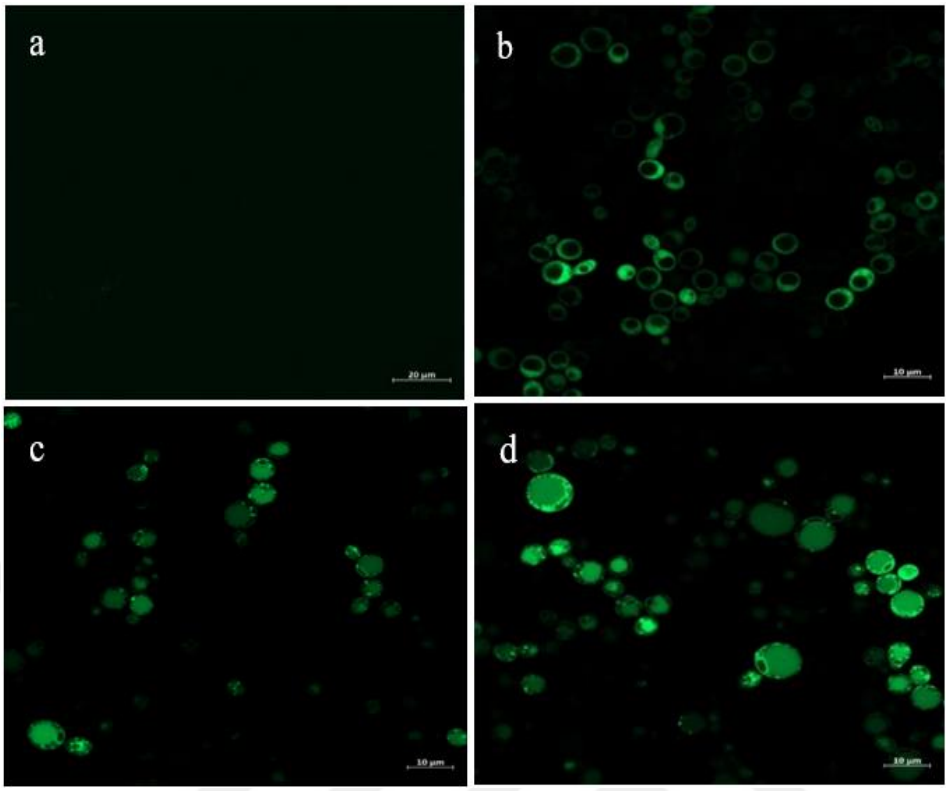

Figure 4.15. Confocal Microscopy Images; **a)** ZHY3-EV (negative control); **b)** ZHY3-GFP (positive control); **c, d)** ZHY3-PdZIP8 fusion

4.6. Determination of the Zinc Uptake of PdZIP8 in Arabidopsis thaliana

4.6.1. Arabidopsis Growth Conditions and Selection of the Homozygous Lines

100 seeds from Col-0 (WT), Col-0 harboring pGFPGUS+ (mock) and *PdZIP8*-overexpressing lines (7-1, 11-2, 12-3) were selected through antibiotic resistance screening. *PdZIP8*-overexpressing T3 lines and mock plantlets exhibited homozygous segregation, while the Col-0 seeds without transformation could not survive in the presence of hygromycin in Murashige and Skoog (MS) medium, confirming the effectiveness of the selection and the absence of the resistance gene in WT plants.

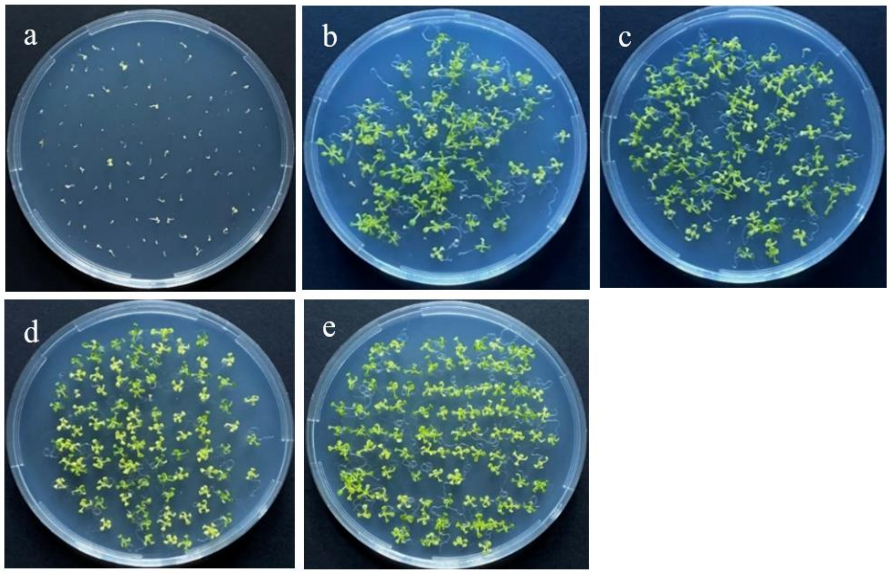

Figure 4.16. Antibiotics selection profile of; **a)** WT; **b)** mock; **c)** line 7-1; **d)** line 11-2; **e)** line 12-3

Table 4.1. Antibiotic selection table of the selected T3 *PdZIP8* lines

Lines	Germinated Seeds	Antibiotic-selected plants
7-1	92	91
11-2	99	91
12-3	100	100

4.6.2. Confirmation of the Presence of the *PdZIP8* Gene via PCR

DNA was isolated from both transgenic and WT Arabidopsis plants, and PCR was conducted using gene-specific primers. WT plants served as the negative control. The region amplified by the PdZIP8-F and PdZIP8-R primers was expected to be 1514 bp. Arabidopsis transgenic lines 7-1, 11-2, and 12-3 exhibited a clear band of the expected size, confirming the presence of the *PdZIP8* gene in their genomic DNA. In contrast, no band was observed in the WT plants, indicating the absence of the *PdZIP8* gene.

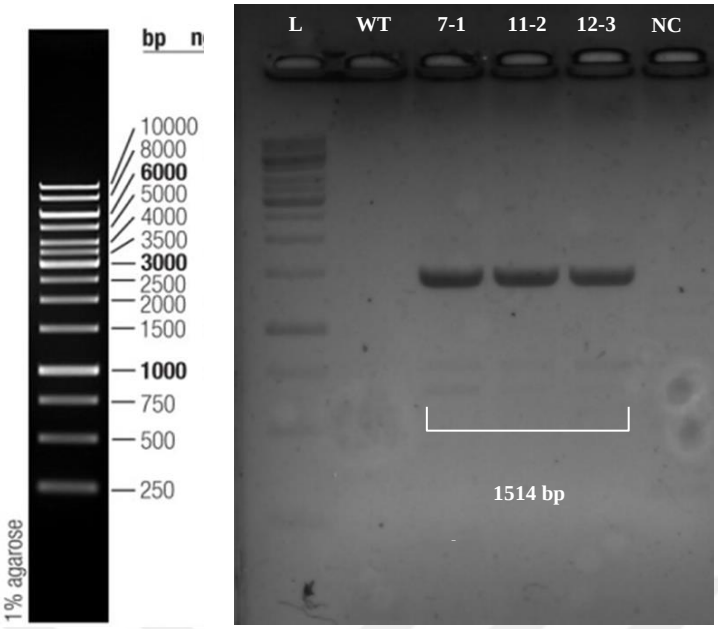

Figure 4.17. Gel image of the PCR samples of WT and *PdZIP8*-overexpressing arabidopsis lines

4.6.3. Real Time Quantitative PCR (RT-qPCR) Analysis of *PdZIP8*-Overexpressing Arabidopsis Lines

The expression of *PdZIP8* was evaluated in transgenic Arabidopsis lines (7-1, 11-2, and 12-3) and compared to WT Col-0 using real time quantitative PCR (RT-qPCR). Expression levels were normalized using *PDF2* as the reference gene. As expected, Col-0, which does not contain the transgene, exhibited a negligible expression level, with a -ΔCt value of-11.43. In contrast, all transgenic lines displayed substantial expression of *PdZIP8*, with -ΔCt values of 5.58, 3.21, and 2.53 for lines 7-1, 11-2, and 12-3, respectively (Figure 4.19). These results confirm the successful overexpression of the *PdZIP8* gene in the transgenic lines.

Among the three lines, 7-1 showed the highest expression level, followed by 11-2 and 12-3. The variation in expression may be attributed to differences in transgene copy number or insertion site effects. RT-qPCR was performed using three biological and three technical replicates to ensure consistency and reliability of the data. This confirmation of transgene expression supports the use of these lines for subsequent analyses aimed at understanding the functional role of *PdZIP8* in metal homeostasis.

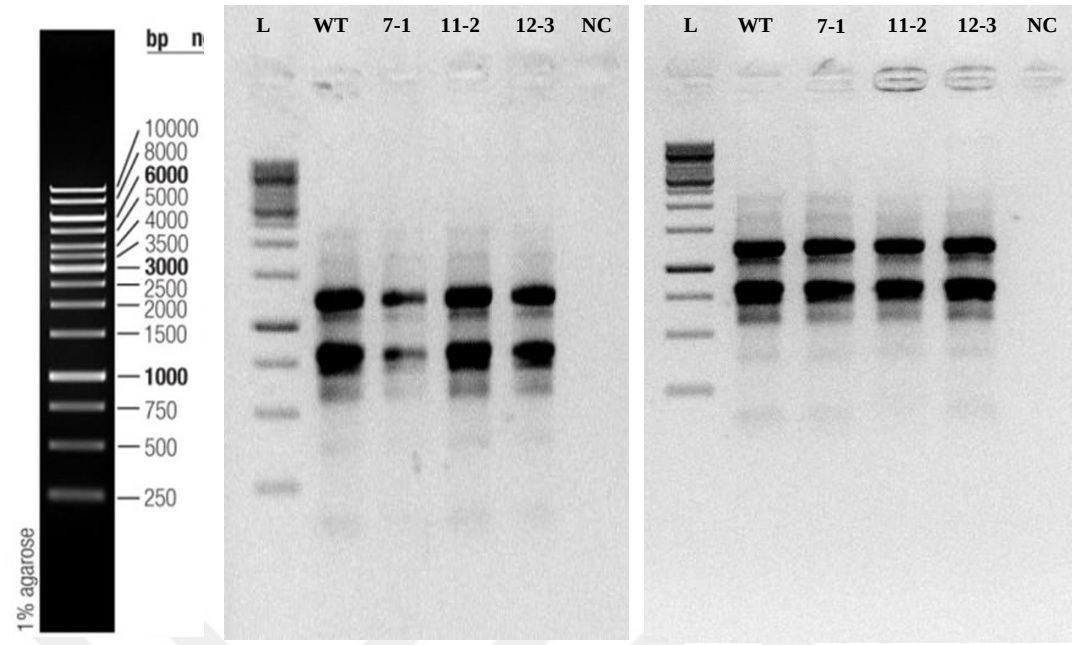

Figure 4.18. Gel images of isolated RNA from WT and T3 lines. (Left: RNA without DNase treatment, Right: RNA after DNase treatment)

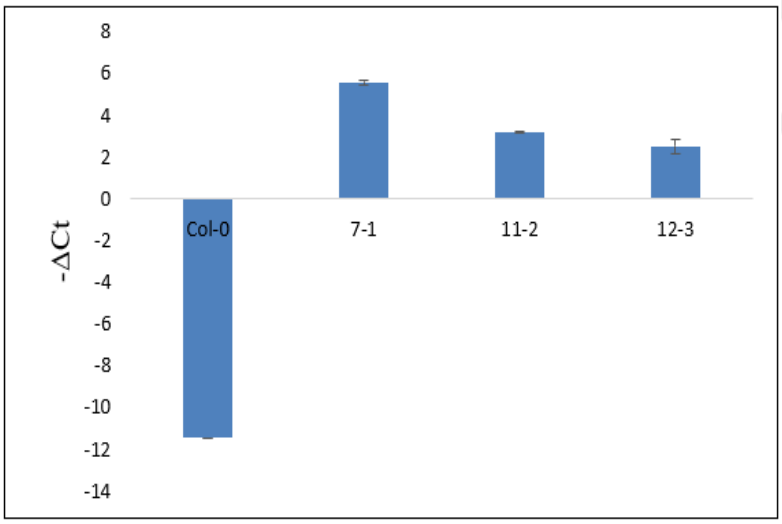

Figure 4.19. Expression levels of *PdZIP8*-overexpressing lines **(**error bars represent the standard deviation of the mean)

4.6.4. Phenotypic Characterization of *PdZIP8*-Overexpressing and Wild-Type Arabidopsis Lines

Under all tested conditions, *PdZIP8*-overexpressing transgenic lines exhibited enhanced root and leaf growth compared to the WT (Col-0), with line 12-3 consistently showing the most vigorous development. WT plants were notably more affected by zinc and iron deficiency, displaying reduced growth, while transgenic lines maintained better performance under micronutrient-limited conditions. These observations suggest that *PdZIP8* functions as a dual zinc and iron transporter, contributing to improved seedling growth by enhancing micronutrient uptake or homeostasis under both sufficient and deficient conditions. The consistent growth advantage of the transgenic lines indicates a positive effect of *PdZIP8* expression on overall plant vigor. These results support the potential role of *PdZIP8* in metal stress tolerance and nutrient acquisition.

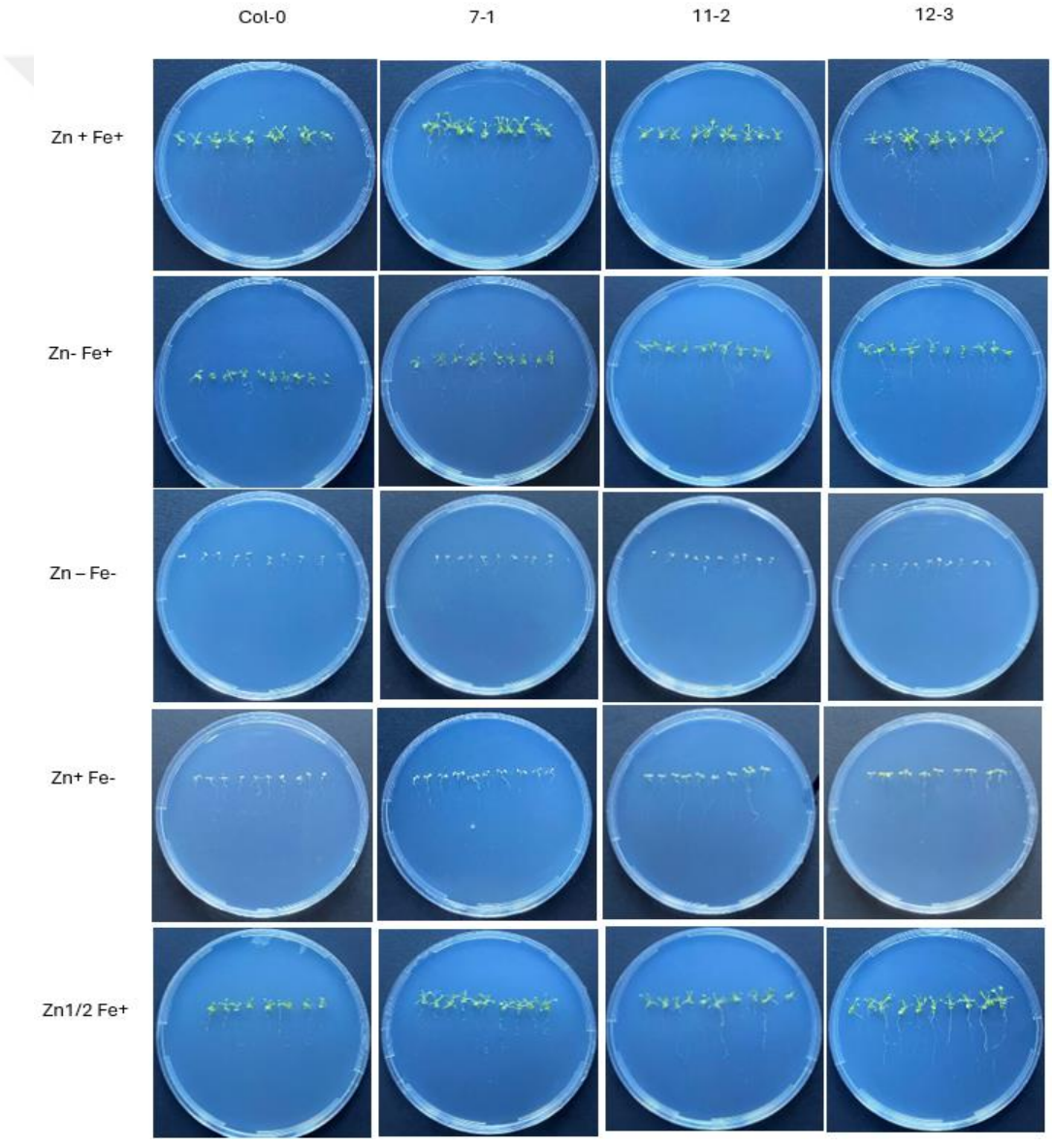

Figure 4.20. Growth trends of WT and *PdZIP8*-overexpressing Arabidopsis lines

PdZIP8-overexpressing lines (11-2 and 12-3) exhibited significantly longer root lengths than Col-0 under both iron-deficient (0 µM $FeSO_4$) and iron-sufficient (100 µM $FeSO_4$) conditions. In iron deficiency, transgenic lines maintained over 2-fold greater root elongation, while Col-0 showed restricted growth. Under sufficient iron, the difference remained with approximately 1.1-fold increase. These results suggest that *PdZIP8* enhances root growth, particularly under low-iron conditions, possibly by improving iron uptake or internal distribution.

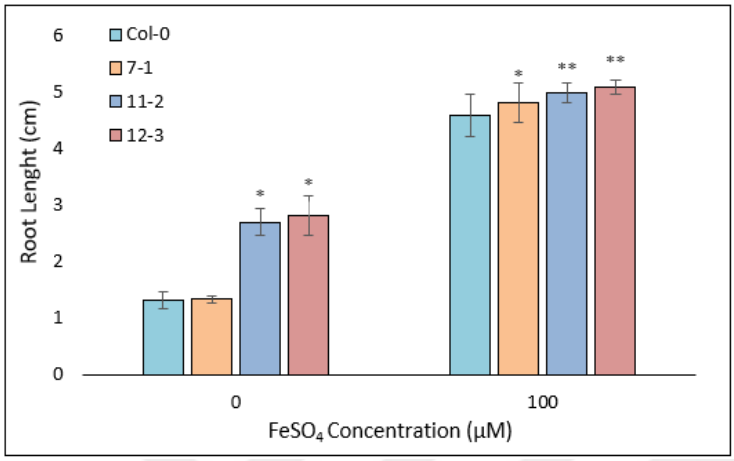

Figure 4.21. Root lengths of Col-0 and *PdZIP8*-overexpressing Arabidopsis lines grown on modified MS medium with 0 or 100 µM $FeSO_4$. Bars show mean root lengths ± SD from three biological replicates. Statistical differences between transgenic lines and Col-0 within each iron condition were assessed by one-way ANOVA with Tukey's test (*$p \leq 0.05$, **$p \leq 0.01$, ***$p \leq 0.001$)

PdZIP8-overexpressing lines exhibited significantly longer root lengths compared to Col-0 at all $ZnSO_4$ concentrations tested. In the absence of zinc (0 µM $ZnSO_4$), the transgenic lines showed approximately a 2-fold increase in root length relative to Col-0. At 15 µM $ZnSO_4$, the difference became more pronounced, reaching up to a 2.3-fold increase. Even under zinc-sufficient conditions (30 µM $ZnSO_4$), *PdZIP8*-overexpressing lines maintained longer roots, with a approximately 1.2-fold increase compared to Col-0. These results indicate that *PdZIP8* overexpression promotes root growth consistently across varying zinc levels, with the most substantial effect observed under moderate zinc supply. This enhancement in root elongation may be linked to improved zinc homeostasis, which can influence auxin signaling and other hormone-regulated pathways involved in root development.

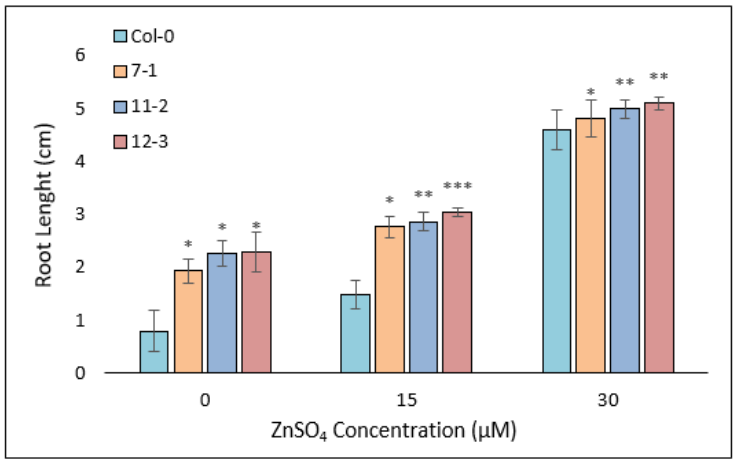

Figure 4.22. Root lengths of Col-0 and *PdZIP8*-overexpressing Arabidopsis lines grown on modified MS medium with 0, 15, or 30 µM $ZnSO_4$. Bars show mean root lengths ± SD from three biological replicates. Statistical differences between transgenic lines and Col-0 within each zinc condition were determined by one-way ANOVA with Tukey's test (*p ≤ 0.05, **p ≤ 0.01, ***p ≤ 0.001)

Leaf lengths of Col-0 and *PdZIP8*-overexpressing Arabidopsis lines were measured. Under iron deficiency (0 µM), all genotypes showed reduced leaf lengths, with transgenic lines with a slight but significant increase compared to Col-0. Under sufficient iron (100 µM $FeSO_4$), *PdZIP8*-overexpressing plants, especially lines 11-2 and 12-3, showed a 4- to 5-fold increase and significantly longer leaves than Col-0. This improvement may result from increased iron uptake or homeostasis mediated by *PdZIP8*, supporting efficient chlorophyll synthesis and growth.

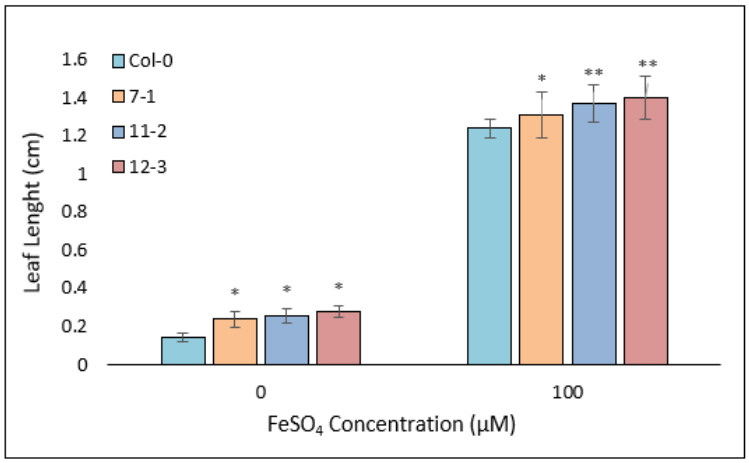

Figure 4.23. Leaf lengths of Col-0 and *PdZIP8*-overexpressing Arabidopsis lines grown on modified MS medium 0 or 100 µM $FeSO_4$. Bars show mean root lengths ± SD from three biological replicates. Statistical differences between transgenic lines and Col-0 within each iron condition were assessed by one-way ANOVA with Tukey's test (*p ≤ 0.05, **p ≤ 0.01, ***p ≤ 0.001)

Leaf length was significantly increased in *PdZIP8*-overexpressing lines compared to Col-0 at all $ZnSO_4$ concentrations. Under zinc deficiency (0 µM), line 12-3 showed the greatest enhancement, with a 2-fold increase relative to Col-0. At 15 µM $ZnSO_4$, leaf lengths of transgenic lines were approximately 1.4- to 1.8-fold longer than Col-0, with line 12-3 again showing the highest increase. Even at zinc-sufficient levels (30 µM), overexpressing lines maintained longer leaves. This growth promotion may be attributed to enhanced zinc uptake and improved zinc-dependent physiological processes mediated by *PdZIP8* overexpression.

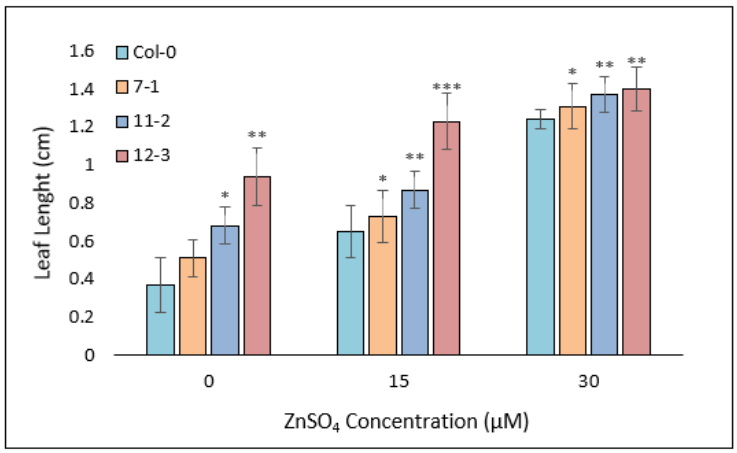

Figure 4.24. Leaf lengths of Col-0 and *PdZIP8*-overexpressing Arabidopsis lines grown on modified MS medium with 0, 15, or 30 µM $ZnSO_4$. Bars show mean root lengths ± SD from three biological replicates. Statistical differences between transgenic lines and Col-0 within each zinc condition were determined by one-way ANOVA with Tukey's test (*$p \leq 0.05$, **$p \leq 0.01$, ***$p \leq 0.001$).

4.6.5. Metal Element Analysis and Measurements of the Fresh and Dry Weights of WT and *PdZIP8* Overexpressing Arabidopsis Lines

Zinc and iron contents of the WT and *PdZIP8*-overexpressing lines grown on modified MS medium supplemented with 10 and 30 µM $ZnSO_4$ were determined using ICP-MS. Both zinc and iron concentrations differed significantly between line 12-3 and the WT, showed a slight but statistically significant difference between line 11-2 and the WT, and were not significantly different between line 7-1 and the WT. This enhanced uptake may result from elevated *PdZIP8* expression levels in line 12-3, promoting more efficient metal transport across cellular membranes. The increase in both zinc and iron accumulation implies that *PdZIP8* may function as a dual-metal transporter or indirectly regulate shared metal uptake pathways.

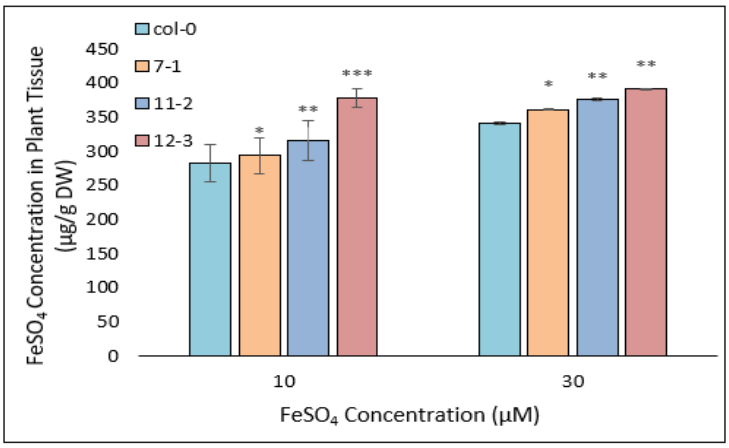

Figure 4.25. Iron concentrations of Col-0 and *PdZIP8*-overexpressing lines (values represent means ± SE (n =3): Statistical significance was determined using one-way ANOVA followed by Tukey's multiple comparison test. Comparisons were made between each transgenic line and Col-0 within each iron concentration. Asterisks indicate statistically significant differences: $p \leq 0.05$: *; $p \leq 0.01$: **; $p \leq 0.001$: ***)

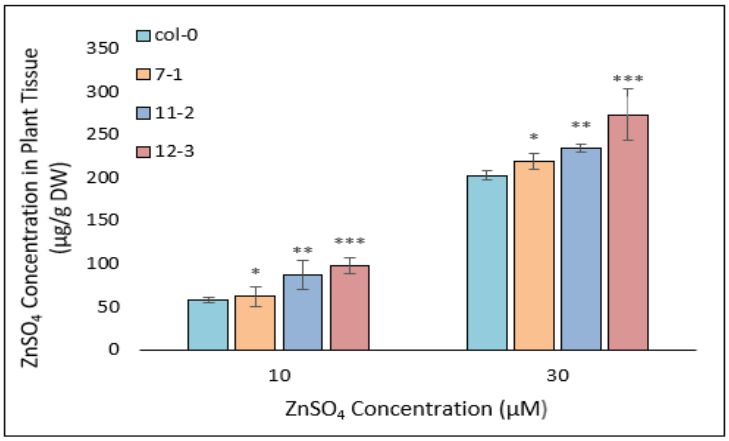

Figure 4.26. Zinc concentrations of Col-0 and *PdZIP8*-overexpressing lines (values represent means ± SE (n =3): Statistical significance was determined using one-way ANOVA followed by Tukey's multiple comparison test. Comparisons were made between each transgenic line and Col-0 within each zinc concentration. Asterisks indicate statistically significant differences: $p \leq 0.05$: *; $p \leq 0.01$: **; $p \leq 0.001$: ***)

Fresh weights of the WT and *PdZIP8*-overexpressing Arabidopsis lines were measured using 15 plantlets per biological replicate, with three biological replicates analyzed per line, as shown in Figure 4.27 and Figure 4.28. All overexpressing lines exhibited significantly greater fresh weight than the WT, with line 12-3 showing the highest increase, followed by lines 11-2 and 7-1. These results suggest that overexpression of *PdZIP8* contributes to accelerated tissue development, resulting in increased fresh biomass. Under zinc-deficient conditions (0 µM $ZnSO_4$), line 12-3 exhibited approximately a 2.5-fold increase in fresh weight compared to Col-0, whereas at 10 µM $ZnSO_4$, the fresh weight of line 12-3 was nearly 3-fold higher than that of the WT. Similarly, under iron deficiency (0 µM $FeSO_4$), line 12-3 showed a 1.6-fold

increase. Even under micronutrient-sufficient conditions, all transgenic lines maintained a moderate but significant increase (1.1–1.2-fold), indicating that *PdZIP8* overexpression enhances plant growth particularly under zinc- and iron-limited conditions.

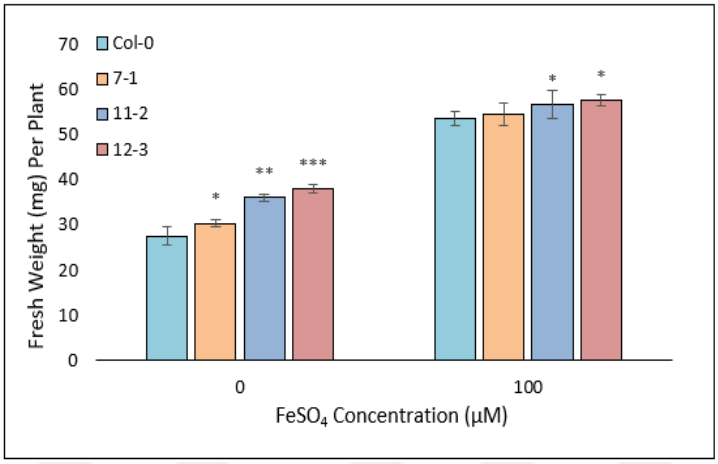

Figure 4.27. Fresh weights of Col-0 and *PdZIP8*-overexpressing plants on modified MS medium with 0 or 100 µM $FeSO_4$. (Values represent means ± SE (n =3). Statistical significance was determined using one-way ANOVA followed by Tukey's multiple comparison test. Comparisons were made between each transgenic line and the Col-0 within each iron concentration. Asterisks indicate statistically significant differences: $p \leq 0.05$: *; $p \leq 0.01$: **; $p \leq 0.001$: ***)

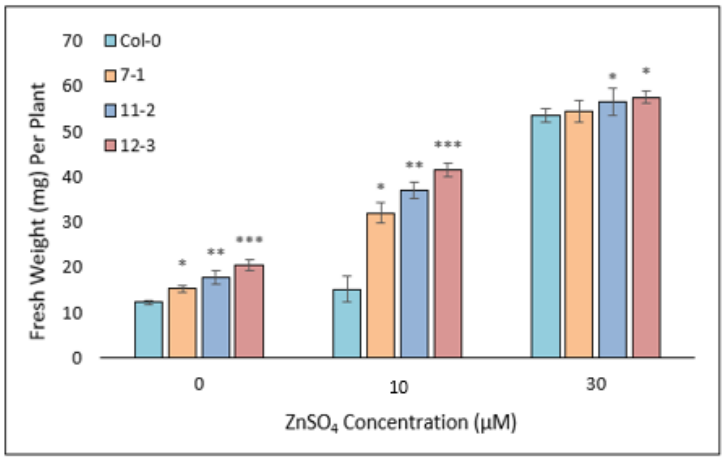

Figure 4.28. Fresh weights of Col-0 and *PdZIP8*-overexpressing lines grown on modified MS medium with 0, 10, or 30 µM $ZnSO_4$. (Values represent means ± SE (n =3). Statistical significance was determined using one-way ANOVA followed by Tukey's multiple comparison test. Comparisons were made between each transgenic line and Col-0 within each zinc concentration. Asterisks indicate statistically significant differences: $p \leq 0.05$: *; $p \leq 0.01$: **; $p \leq 0.001$: ***)

Similarly, dry weights of the same lines were assessed and are presented in Figure 4.29 and Figure 4.30. Consistent with the fresh weight results, all *PdZIP8*-overexpressing lines displayed significantly higher dry biomass than the WT. Among

the transgenics, line 12-3 again exhibited the greatest increase, with lines 11-2 and 7-1 showing moderate enhancements. The increased biomass observed in *PdZIP8*-overexpressing lines may be attributed to improved zinc and iron uptake and homeostasis.

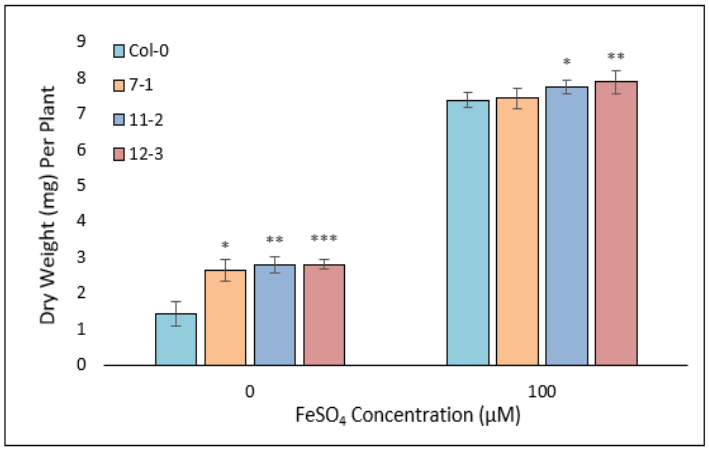

Figure 4.29. Dry weights of Col-0 and *PdZIP8*-overexpressing plants on modified MS medium with 0 or 100 µM $FeSO_4$. (Values represent means ± SE (n =3). Statistical significance was determined using one-way ANOVA followed by Tukey's multiple comparison test. Comparisons were made between each transgenic line and the Col-0 within each iron concentration. Asterisks indicate statistically significant differences: $p \leq 0.05$: *; $p \leq 0.01$: **; $p \leq 0.001$: ***)

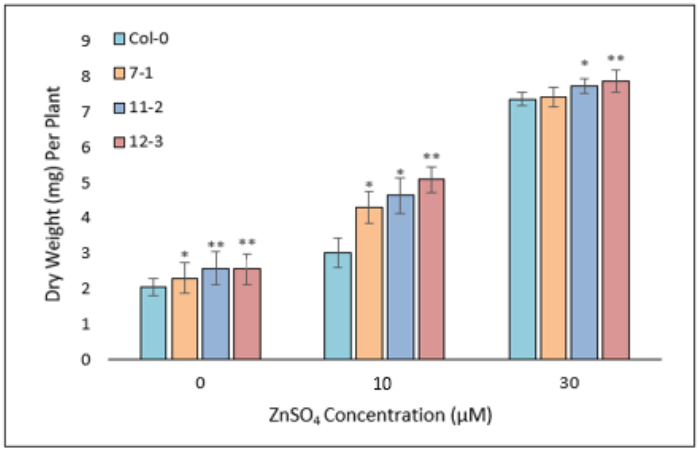

Figure 4.30. Dry weights of Col-0 and *PdZIP8*-overexpressing plants on modified MS medium with 0, 10, or 30 µM $ZnSO_4$. (Values represent means ± SE (n =3). Statistical significance was determined using one-way ANOVA followed by Tukey's multiple comparison test. Comparisons were made between each transgenic line and the Col-0 within each zinc concentration. Asterisks indicate statistically significant differences: $p \leq 0.05$: *; $p \leq 0.01$: **; $p \leq 0.001$: ***)

4.6.6. Measurements of Chlorophyll Concentrations in WT and *PdZIP8*-Overexpressing Arabidopsis Lines

To further assess the role of the *PdZIP8* gene in chlorophyll content, the total chlorophyll concentration (chlorophyll a + b) was measured in WT and *PdZIP8*-overexpressing lines grown under different iron conditions. Under iron-deficient conditions (0 µM $FeSO_4$), all *PdZIP8*-overexpressing lines exhibited significantly higher chlorophyll concentrations than Col-0, with line 12-3 showing the highest levels, approximately a 2-fold increase compared to Col-0. Upon iron supplementation (100 µM $FeSO_4$), chlorophyll content increased in all genotypes, but transgenic lines still maintained a slight advantage with up to 1.1-fold higher levels. These findings suggest that *PdZIP8* plays a critical role in maintaining chlorophyll content under iron-limited conditions, potentially by enhancing metal uptake or homeostasis, which supports chlorophyll biosynthesis or stability.

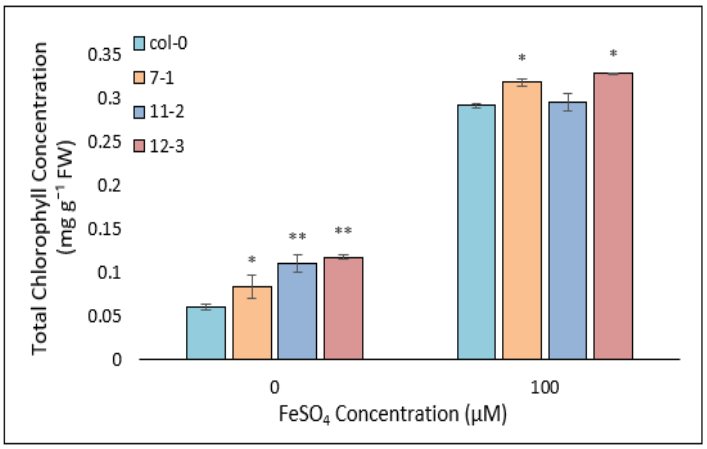

Figure 4.31. Total chlorophyll concentrations in Col-0 and *PdZIP8*-overexpressing lines grown on modified MS medium containing 0 or 100 µM $FeSO_4$. (Values represent means ± SE (n =3). Statistical significance was determined using one-way ANOVA followed by Tukey's multiple comparison test. Comparisons were made between each transgenic line and Col-0 within each iron concentration. Asterisks indicate statistically significant differences: $p \leq 0.05$: *; $p \leq 0.01$: **; $p \leq 0.001$: ***)

Similarly, total chlorophyll content was evaluated in WT and *PdZIP8*-overexpressing lines under varying zinc concentrations to further clarify PdZIP8's role. Under zinc deficiency (0 µM $ZnSO_4$), *PdZIP8*-overexpressing lines showed significantly higher chlorophyll concentrations than Col-0, with line 12-3 reaching approximately 1.4-fold higher levels. This enhancement was consistent at 15 µM and 30 µM $ZnSO_4$, where transgenic lines accumulated up to 1.2- to 1.3-fold more chlorophyll than Col-0. These results reinforce the conclusion that *PdZIP8* positively influences chlorophyll content under both zinc-deficient and zinc-sufficient conditions, likely by contributing to improved zinc uptake and physiological balance.

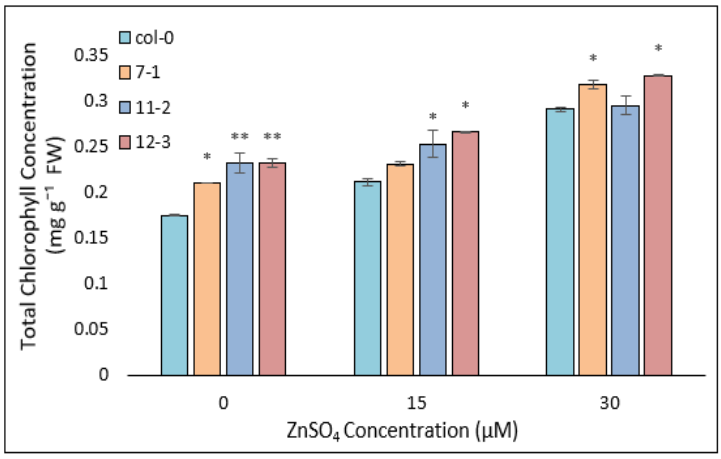

Figure 4.32. Total chlorophyll concentrations in Col-0 and *PdZIP8*-overexpressing lines grown on modified MS medium with 0, 15, or 30 µM $ZnSO_4$. (Values represent means ± SE (n =3). Statistical significance was determined using one-way ANOVA followed by Tukey's multiple comparison test. Comparisons were made between each transgenic line and Col-0 within each zinc concentration. Asterisks indicate statistically significant differences: $p \leq 0.05$: *; $p \leq 0.01$: **; $p \leq 0.001$: ***)

5.DISCUSSION

Zinc deficiency is a widespread issue that adversely affects both agricultural productivity and human health. Insufficient zinc levels result in notable reductions in plant yield and quality, while also resulting various health complications in individuals. To prevent the effects of zinc deficiency in plants, it is crucial to gain a comprehensive understanding of the mechanisms underlying zinc uptake and to identify the genes involved in its absorption. Zinc Regulated- Iron Regulated Transporters (ZIPs) have a significant role in zinc influx into cells. Although several ZIPs have been characterized in various plant species, to date no ZIP gene has been functionally characterized in *P. distans* under zinc deficiency. This thesis hypothesizes that *PdZIP8* is a key transporter gene in *P. distans*, encoding a protein involved in the cellular uptake of zinc, especially under zinc deficient conditions. The functional characterization of *PdZIP8* is essential for understanding how *P. distans* and other related species manage zinc homeostasis. By studying the expression, localization, and functional role of *PdZIP8*, this research aims to provide valuable insights into its involvement in zinc uptake and transport.

Yeast complementation assay is considered one of the most important step in the functional characterization of various studies. For instance, Kozak et al. (2018), performed a complementation assay to investigate the zinc uptake function of *NtZIP11*. The zinc uptake mutant yeast strain ZHY3 and the wild type strain DY1453 were used for the study. EGTA was added to the yeast growth media to establish zinc deficiency conditions. It was concluded that ZHY3 cells transformed with the empty vector were unable to grow at a concentration of 5 mM EGTA. However, ZHY3 cells transformed with vector harboring *NtZIP1* gene were able to complement the deficiency and grow even at a concentration of 7.5 mM EGTA. Similarly, Coninx et al. (2019) reported that the *SlZRT1* gene is involved in zinc homeostasis, as ZHY3 cells transformed with *SlZRT1* gene were able to complement the concentration of 200 µM EDTA.

Consistent with the previous studies, in the present study, *PdZIP8* harboring yeast expression vector was transformed to W303 and ZHY3 yeast strains. Empty vector was used as a control to evaluate the complementation ability of the gene. EDTA and EGTA chelating agents were added to selective yeast growth media to create zinc deficient environment. Although ZHY3 is a mutant strain and could not grow under zinc deficiency, *PdZIP8* reversed the growth defect of zinc uptake mutants in yeast. Consequently, PdZIP8-containing cells were able to grow at concentrations of 200 µM EDTA and 20 mM EGTA, whereas ZHY3 cells transformed with the empty vector could only grow at 10 µM EDTA and 12.5 mM EGTA. These findings indicate that *PdZIP8* possess the capability to complement zinc deficiency.

Subcellular localization refers to the specific localization of proteins within a cell and provides critical insights into their potential functions. To investigate the subcellular localization of the encoded protein, *PdZIP8* was fused with pAG426GPD-EGFP vector and the resultant PdZIP8-GFP construct was transformed into the ZHY3 yeast strain. Interestingly, it was observed that PdZIP8 protein localizated to the plasma membrane and endoplasmic reticulum (ER) This finding contradicts with previous studies suggesting that transporters are primarily localized to the plasma membrane of the cell (Milner et al. 2012; Tiong et al. 2013; Lee et al. 2015). However, Durmaz et al. (2011) reported that the TdZIP1 transporter protein localized to the ER membrane

which aligns with our findings. Nishida et al. (2008) identified *ZNT1* as a zinc transporter in *Thlaspi japonicum*. Nevertheless, TjZNT1 was localized to the plasma membrane as well as the other organelles of the cell. Furthermore, Li et al (2015) and Liu et al. (2019) demonstrated that ZmZIP3 and OsZIP1 localized to the plasma membrane and endoplasmic reticulum in arabidopsis and rice protoplasts, respectively. One possible explanation for the observed localization of PdZIP8-GFP to the plasma membrane and ER may be the improper protein folding, which could prevent its proper location on plasma membrane. Alternatively, the mistargeted localization could suggest that PdZIP8 plays a role in the subcellular transport of zinc rather than in an extracellular compartment, particularly within the ER to maintain essential cellular functions such as degradation, secretion and protein folding.

Analyzing the expression levels of *PdZIP8* in overexpressing Arabidopsis lines by RT-qPCR and evaluating the impact of *PdZIP8* under zinc-deficiency conditions are crucial aspects of this study, both phenotypically and quantitatively. For the phenotypic analysis, leaf and root lengths of three *PdZIP8*-overexpressing Arabidopsis lines were measured as indicators of plant growth and development, and compared with WT and mock lines. For the quantitative analysis, the zinc content in both transgenic and WT plants was determined using ICP-MS, providing precise measurements of zinc accumulation. Additionally, chlorophyll content was assessed.

Lee et al. (2010) functionally characterized *OsZIP8* by generating overexpressing rice plants. The overexpression of *OsZIP8* was induced under Zn deficiency. It was observed that zinc concentrations in roots were higher in the transgenics than in WT irrespective of external Zn status, whereas zinc concentrations in shoots and seeds were lower in the transgenics compared with WT. In contrast to their findings, where zinc concentrations were higher in the roots but lower in the shoots and seeds of OsZIP8-overexpressing rice plants, our study presents a different outcome regarding plant growth. In our study, overexpression of *PdZIP8* led to increased root and shoot lengths in the transgenic plants compared to WT plants.

Notably, Li et al. (2015) reported that transgenic Arabidopsis plants overexpressing *ZmZIP3* exhibited better tolerance to various zinc conditions (0, 30 µM, and 200 µM $ZnSO_4$) compared to WT plants, particularly under excess zinc conditions, as their roots and leaves were longer than those of WT plants. Similarly, our study observed increased root and shoot lengths in transgenic plants overexpressing *PdZIP8*, indicating that both transporters may enhance plant growth and tolerance to varying zinc levels. Likewise *ZmZIP3*, they characterized another zinc transporter gene, *ZmZIP7*, in Arabidopsis (2016). ZmZIP7-overexpressing Arabidopsis lines were generated and the metal contents in transgenic and WT plants were examined using ICP-MS. It was concluded that ZmZIP7 encodes a functional zinc and iron transporter, and ectopic overexpression of *ZmZIP7* in Arabidopsis stimulate endogenous iron and zinc uptake mechanisms, thereby facilitating both metal uptake and homeostasis.

Ma et al. (2019) identified 18 *MaZIP* genes in apple (*Malus domestica* L.) and cloned *MaZIP10*, which was subsequently transformed into Arabidopsis. The expression of *MaZIP10* was induced under both zinc and iron deficiency conditions. Transgenic plants overexpressing *MdZIP10* accumulated higher levels of zinc and iron in their shoots and roots compared to WT plants. The overexpression of *MdZIP10*

alleviated zinc deficiency symptoms, and the transgenic plants exhibited significantly longer roots than WT plants under standard conditions. These findings align with the results observed in our study. However, they reported no significant differences in the expression of *MdZIP10* between WT and transgenic lines when exposed to excess zinc, which contrasts with our findings.

Another finding is that Lee et al. (2021) characterized three ZIP transporters from Arabidopsis (ZIP4, ZIP6, ZIP9) to understand their functions. It was demonstrated that ZIP proteins can restore the growth defect of a yeast zinc uptake mutant and are upregulated under zinc deficiency. Furthermore, it was confirmed that the expression of all three genes is induced in roots when plants are grown under zinc deficient conditions. To characterize further the functional role of each ZIP gene in regulating zinc homeostasis, T-DNA mutants for ZIP genes were isolated. The *zip4-2*, *zip4-3*, *zip6-1*, *zip6-2*, and *zip9* mutants were loss-of-function mutants with no detectable expression. When grown on zinc containing medium, no obvious phenotypic differences were observed between the T-DNA mutants and WT plants, with similar fresh weight and root length. Under Zn deficiency, the T-DNA mutants exhibited growth similar to WT plants, as indicated by comparable biomass and root length. Analysis of zinc distribution revealed that, compared to WT, the mutants accumulated similar levels of zinc in both shoots and roots under both zinc sufficient and zinc deficient conditions, reflecting the lack of significant phenotypic differences.

Gu et al. (2021) identified six ZIPs from blueberry genome (*VcZIP1*, *VcZIP2*, *VcZIP6*, *VcZIP7*, *VcZIP8* and *VcZIP11*) and transformed them in Arabidopsis. The overexpression of identified VcZIP genes was altered, with some genes such as *VcZIP1* and *VcZIP6* being upregulated in response to the zinc deficiency. The results of expression patterns, yeast complementation tests and the transgenic experiments indicated that VcZIP1, VcZIP7, VcZIP8 and VcZIP11 are responsible for zinc transport, VcZIP1 and VcZIP7 for cadmium transport, and VcZIP6, VcZIP7 and VcZIP8 for iron transport. This suggests that ZIPs facilitate the uptake of not only zinc but also other divalent metals, such as cadmium and iron.

As observed in many previous studies, while there may be slight differences due to experimental variations and technical approaches, the core results and methodologies remain largely consistent. In this study, *PdZIP8* was shown to exhibit zinc transporter functions through a variety of methods, including yeast complementation assays, phenotypic analysis in overexpressing transgenic lines, zinc quantification using ICP-MS, and chlorophyll content analysis. Each of these approaches provided complementary evidence that *PdZIP8* plays a key role in zinc uptake, particularly under zinc deficiency conditions. The yeast complementation assays confirmed its ability to restore growth in zinc deficient yeast, while the phenotypic analysis revealed enhanced root and leaf growth in transgenic plants comparing with WT plants. Additionally, zinc content quantification and chlorophyll analysis further supported its involvement in zinc accumulation and in preventing chlorosis. Taken together, these results strongly suggest that PdZIP8 functions as an essential zinc transporter, contributing to zinc homeostasis and uptake in plants under zinc deficiency conditions.

6. CONCLUSION

Zinc is an essential micronutrient for plants, playing a key role in various biological processes such as enzyme function, protein synthesis, gene expression, and cell division. However, zinc deficiency in soils is a widespread problem that limits plant growth and crop yield. Understanding how plants absorb and regulate zinc is therefore critical for improving agricultural productivity, especially in zinc-deficient environments. Among the main proteins involved in zinc uptake are ZIP transporters. Although many ZIP genes have been identified in different plant species, the specific roles and mechanisms of many remain unclear.

In this study, the ZIP transporter gene *PdZIP8*, identified from *Puccinellia distans*, was functionally characterized using both yeast and plant models. The ability of *PdZIP8* to complement the growth defect of the zinc uptake-deficient yeast mutant ZHY3 under zinc-starved conditions (200 μM EDTA and 20 mM EGTA) confirmed its function as a zinc transporter. This finding provided a strong indication that *PdZIP8* facilitates zinc uptake across cellular membranes.

To further investigate its role in planta, *PdZIP8* was overexpressed in *Arabidopsis thaliana*. Transgenic lines (especially line 12-3) exhibited improved growth compared to the wild type under zinc-deficient conditions. These lines showed significantly longer roots and larger leaves, suggesting better adaptation to nutrient stress. ICP-MS analysis revealed that the transgenic lines accumulated more zinc, and in some cases more iron, than Col-0. These results indicate that *PdZIP8* plays a role not only in zinc uptake but also possibly in influencing iron homeostasis. Increased metal content was associated with higher chlorophyll levels under both zinc- and iron-limited conditions, suggesting that *PdZIP8* contributes to maintaining photosynthetic activity when nutrients are scarce. The enhancement in root growth may be linked to altered auxin-related responses, since zinc availability and auxin signaling are known to interact in root development.

Overall, the study demonstrates that *PdZIP8* is a functional zinc transporter that enhances nutrient uptake and promotes plant growth under zinc- and iron-deficient conditions. The fact that it works effectively in both yeast and *Arabidopsis* confirms its conserved role and supports its potential use in agricultural biotechnology. By introducing genes like *PdZIP8* into crop plants, it may be possible to develop varieties that are more efficient in zinc uptake, better adapted to nutrient-poor soils, and capable of producing higher yields with improved nutritional quality.

Such improvements would be highly beneficial in regions suffering from micronutrient deficiencies and could reduce the need for synthetic fertilizers, leading to cost savings for farmers and reduced environmental impact. The application of *PdZIP8* in future crop improvement strategies offers a promising path toward more sustainable agriculture and enhanced food security. Further research on *PdZIP8* in crop species and under field conditions will help better understand its full potential and guide its use in plant breeding and genetic engineering programs.

7. REFERENCES

Coninx, L., Smisdom, N., Kohler, A., Arnauts, N., Ameloot, M., Rineau, F., Ruytinx, J., 2019. *SlZRT2* encodes a ZIP family Zn transporter with dual localization in the ectomycorrhizal fungus *Suillus luteus*. *Frontiers in Microbiology*, 10, 2251.

Çakmak, İ., Kalaycı, M., Ekiz, H., Braund, H. J., Kılınç, Y., Yılmaz, A., 1999. Zinc deficiency as a practical problem in plant and human nutrition in Turkey: A NATO-science for stability project. *Field Crops Research*, 60, 175-188.

Çakmak, İ., Marschner, H., Bangerth, F., 1989. Effect of zinc nutritional status on growth, protein metabolism and levels of indole-3-acetic acid and other phytohormones in bean (*Phaseolus vulgaris* L.). *Journal of Experimental Botany*, 40, 405-412.

Doyle, J. (1991). DNA protocols for plants. In *Molecular techniques in taxonomy* (pp. 283-293). Berlin, Heidelberg: Springer Berlin Heidelberg.

Durmaz, E., Coruh, C., Dinler, G., Grusak, M. A., Peleg, Z., Saranga, Y., Budak, H., 2011. Expression and cellular localization of ZIP1 transporter under zinc deficiency in wild emmer wheat. *Plant Molecular Biology Reporter*, 29, 582-596.

Eide, D., Broderius, M., Fett, J., Guerinot, M. L., 1996. A novel iron-regulated metal transporter from plants identified by functional expression in yeast. *Proceedings of the National Academy of Sciences*, 93, 5624-5628.

Eyüpoğlu, F., Kurucu, N., & Talaz, S., 1996. Türkiye topraklarının bitkiye yarayışlı bazı mikroelementler bakımından genel durumu. *Toprak Gübre Araştırma Enstitüsü Yayınları, Ankara*.

FAO, 2000. Calcareous Soils. FAO AGL Land and Plant Nutrition Management Services. Retrieved from: www.fao.org/ag/agl/agll/prosoil/calc.htm [February 24, 2009]

Fu, X. Z., Zhou, X., Xing, F., Ling, L. L., Chun, C. P., Cao, L., 2017. Genome-wide identification, cloning and functional analysis of the zinc/iron-regulated transporter-like protein (ZIP) gene family in trifoliate orange (*Poncirus trifoliata* L. Raf.). *Frontiers in Plant Science*, 8, 588.

Gaither, L. A., Eide, D. J., 2001. Eukaryotic zinc transporters and their regulation. *Zinc Biochemistry, Physiology, and Homeostasis: Recent Insights and Current Trends*, 65-84.

Gainza-Cortés, F., Pérez-Dïaz, R., Pérez-Castro, R., Tapia, J., Casaretto, J. A., González, S., González, E., 2012. Characterization of a putative grapevine Zn transporter, VvZIP3, suggests its involvement in early reproductive development in *Vitis vinifera* L. *BMC Plant Biology*, 12, 1-13.

Gao, F., Li, J., Zhang, J., Li, N., Tang, C., Bakpa, E. P., Xie, J., 2022. Genome-wide identification of the ZIP gene family in lettuce (*Lactuca sativa* L.) and expression analysis under different element stress. *Plos One*, 17, e0274319.

Grotz, N., Fox, T., Connolly, E., Park, W., Guerinot, M. L., Eide, D., 1998. Identification of a family of zinc transporter genes from Arabidopsis that respond to zinc deficiency. *Proceedings of the National Academy of Sciences*, 95, 7220-7224.

Grotz, N., Guerinot, M. L., 2006. Molecular aspects of Cu, Fe and Zn homeostasis in plants. *Biochimica et Biophysica Acta (BBA)-Molecular Cell Research*, 1763, 595-608.

Gu, J., Xu, J., Guo, Y., Zong, Y., Chen, W., & Guo, W. (2021). Cloning and functional analysis of ZIP transporters in blueberry. *Scientia Horticulturae*, *278*, 109871.

Guerinot, M. L., 2000. The ZIP family of metal transporters. *Biochimica et Biophysica Acta (BBA)-Biomembranes*, 1465, 190-198.

Guerinot, M. L., Eide, D., 1999. Zeroing in on zinc uptake in yeast and plants. *Current Opinion in Plant Biology*, 2, 244-249.

Gupta, N., Ram, H., Kumar, B., 2016. Mechanism of zinc absorption in plants: uptake, transport, translocation and accumulation. *Reviews in Environmental Science and Bio/Technology*, 15, 89-109.

Hambidge, M., 2000. Human zinc deficiency. *The Journal of Nutrition*, 130, 1344-1349.

He, L., Girijashanker, K., Dalton, T. P., Reed, J., Li, H., Soleimani, M., Nebert, D. W., 2006. ZIP8, member of the solute-carrier-39 (SLC39) metal-transporter family: characterization of transporter properties. *Molecular Pharmacology*, 70, 171-180.

Ishimaru, Y., Suzuki, M., Kobayashi, T., Takahashi, M., Nakanishi, H., Mori, S., 2005. OsZIP4, a novel zinc-regulated zinc transporter in rice. *Journal of Experimental Botany*, 56, 3207–3214.

Kochian, L. V., 2000. Molecular physiology of mineral nutrient acquisition, transport, and utilization. *Biochemical and Molecular Biology of Plants*, 20, 1204–1249.

Lee, S., Jeong, H. J., Kim, S. A., Lee, J., Guerinot, M. L., An, G., 2010. OsZIP5 is a plasma membrane zinc transporter in rice. *Plant Molecular Biology*, 73, 507-517.

Lee, S., Kim, S. A., Lee, J., Guerinot, M. L., An, G., 2010. Zinc deficiency-inducible *OsZIP8* encodes a plasma membrane-localized zinc transporter in rice. *Molecules and Cells*, 29, 551-558.

Lee, S., Lee, J., Ricachenevsky, F. K., Punshon, T., Tappero, R., Salt, D. E., & Guerinot, M. L. (2021). Redundant roles of four ZIP family members in zinc homeostasis and seed development in Arabidopsis thaliana. *The Plant Journal*, *108*(4), 1162-1173.

Li, S., Liu, Z., Guo, L., Li, H., Nie, X., Chai, S., Zheng, W., 2019. Genome-wide identification of ZIP gene family members in wheat.

Li, S., Zhou, X., Li, H., Liu, Y., Zhu, L., Guo, J., ... & Chen, R. (2015). Overexpression of ZmIRT1 and ZmZIP3 enhances iron and zinc accumulation in transgenic Arabidopsis. *PloS one*, *10*(8), e0136647.

Li, S., Zhou, X., Zhao, Y., Li, H., Liu, Y., Zhu, L., ... & Chen, R. (2016). Constitutive expression of the ZmZIP7 in Arabidopsis alters metal homeostasis and increases Fe and Zn content. *Plant Physiology and Biochemistry*, *106*, 1-10.

Liu, X. S., Feng, S. J., Zhang, B. Q., Wang, M. Q., Cao, H. W., Rono, J. K., Yang, Z. M., 2019. OsZIP1 functions as a metal efflux transporter limiting excess zinc, copper and cadmium accumulation in rice. *BMC Plant Biology*, 19, 1-16.

Livak, K. J., & Schmittgen, T. D. (2001). Analysis of relative gene expression data using real-time quantitative PCR and the 2− ΔΔCT method. *methods*, *25*(4), 402-408.

López-Millán, A. F., Ellis, D. R., Grusak, M. A., 2004. Identification and characterization of several new members of the ZIP family of metal ion transporters in *Medicago truncatula*. *Plant Molecular Biology*, 54, 583-596.

Ma, X., Liu, H., Cao, H., Qi, R., Yang, K., Zhao, R., ... & Zhang, Y. (2019). Genome-wide analysis of zinc-and iron-regulated transporter-like protein family members in apple and functional validation of ZIP10. *Biometals*, *32*, 657-669.

Mandal, B., Hazra, G. C., Pal, A. K., 1988. Transformation of zinc in soils under submerged condition and its relation with zinc nutrition of rice. *Plant and Soil*, 106, 121–126.

Matheson, K., Parsons, L., & Gammie, A. (2017). Whole-Genome Sequence and Variant Analysis of W303, a Widely-Used Strain of *Saccharomyces cerevisiae*. *G3 (Bethesda, Md.)*, *7*(7), 2219–2226. https://doi.org/10.1534/g3.117.040022

McCall, K. A., Huang, C. C., Fierke, C. A., 2000. Function and mechanism of zinc metalloenzymes. *The Journal of Nutrition*, 130, 1437-1446.

Milner, M. J., Seamon, J., Craft, E., Kochian, L. V., 2013. Transport properties of members of the ZIP family in plants and their role in Zn and Mn homeostasis. *Journal of Experimental Botany*, 64, 369–381.

Mondal, T. K., Ganie, S. A., Rana, M. K., Sharma, T. R., 2013. Genome-wide analysis of zinc transporter genes of maize (*Zea mays*). *Plant Molecular Biology Reports*, 32, 605–616.

Nishida, S., Mizuno, T., Obata, H., 2008. Involvement of histidine-rich domain of ZIP family transporter TjZNT1 in metal ion specificity. *Plant Physiology and Biochemistry*, 46, 601-606.

Pedas, P., Schjoerring, J. K., Husted, S., 2009. Identification and characterization of zinc-starvation-induced ZIP transporters from barley roots. *Plant Physiology and Biochemistry*, 47, 377-383.

Prasad, A. (2013). Trace elements and iron in human metabolism. *Springer Science & Business Media*.

Ramesh, S. A., Shin, R., Eide, D. J., Schachtman, D. P., 2003. Differential metal selectivity and gene expression of two zinc transporters from rice. *Plant Physiology*, 133, 126

Rengel, Z., Römheld, V., Marschner, H., 1998. Uptake of zinc and iron by wheat genotypes differing in tolerance to zinc deficiency. *Journal of Plant Physiology*, 152(4-5), 433-438.

Suzuki, M., Takahashi, M., Tsukamoto, T., Watanabe, S., Matsuhashi, S., Yazaki, J., 2006. Biosynthesis and secretion of mugineic acid family phytosiderophores in zinc−deficient barley. *Plant Journal*, 48, 85–97.

Tapiero, H., Tew, K. D., 2003. Trace elements in human physiology and pathology: zinc and metallothioneins. *Biomedicine & Pharmacotherapy*, 57(9), 399-411.

Tiong, J., McDonald, G., Genc, Y., Shirley, N., Langridge, P., Huang, C. Y., 2015. Increased expression of six ZIP family genes by zinc (Zn) deficiency is associated with enhanced uptake and root−to−shoot translocation of Zn in barley (*Hordeum vulgare*). *New Phytologist*, 207, 1097–1109.

Van De Mortel, J. E., Almar Villanueva, L., Schat, H., Kwekkeboom, J., Coughlan, S., Moerland, P. D., Aarts, M. G., 2006. Large expression differences in genes for iron and

zinc homeostasis, stress response, and lignin biosynthesis distinguish roots of Arabidopsis thaliana and the related metal hyperaccumulator *Thlaspi caerulescens*. *Plant Physiology*, 142(3), 1127-114.

Welch, R. M., Graham, R. D., 2012. Perspectives on enhancing the nutritional quality of food crops with trace elements. *Fertilizing Crops to Improve Human Health: a Scientific Review*, 65.

Yokokawa, H., Morita, Y., Hamada, I., 2024. Demographic and clinical characteristics of patients with zinc deficiency: analysis of a nationwide Japanese medical claims database. *Scientific Reports*, 14, 2791.

Zang, Z. S., Xu, Y. M., Lau, A. T., 2016. Molecular and pathophysiological aspects of metal ion uptake by the zinc transporter ZIP8 (SLC39A8). *Toxicology Research*, 5(4), 987-1002.

Zhao, H., Eide, D., 1996. The yeast *ZRT1* gene encodes the zinc transporter protein of a high-affinity uptake system induced by zinc limitation. *Proceedings of the National Academy of Sciences*, 93(6), 2454-2458.

CURRICULUM VITAE

Beyza YÜKSEL

EDUCATION

MSc 2022-2025	Akdeniz University, Graduate School of Natural and Applied Sciences Agricultural Biotechnology, Antalya
BSc 2017-2022	Niğde Ömer Halisdemir University Agricultural Genetic Engineering, Niğde

ACADEMIC STUDIES

2024- AKDENIZ UNIVERSITY. Assessment of the Developmental Profiles of ZHY3 and W303 Yeast Strains in Zinc-Modified Media